MSc Thesis Biobased Chemistry and Technology

Carbohydrate oxidation by platinum on activated carbon: Altering the catalytic performance by changing the surface chemistry of the support

Marlene Führer

September 2017- March 2018

Supervisors:

Dr. ir. T (Tomas) van Haasterecht
EB (Evie) van der Wijst
Prof. dr. JH (Harry) Bitter

WAGENINGEN
UNIVERSITY & RESEARCH

Carbohydrate oxidation by platinum on activated carbon: Altering the catalytic performance by changing the surface chemistry of the support

Name course	:	MSc Thesis Biobased Chemistry and Technology
Number	:	BCT-80436
Study load	:	36 ects
Date	:	September 2017 – March 2018
Student	:	Marlene Führer
Registration number	:	930817249050
Study programme	:	MBT
Report number	:	092BCT
Supervisor(s)	:	Dr. ir. T (Tomas) van Haasterecht, EB (Evie) van der Wijst MSc & prof. JH (Harry) Bitter
Examiners	:	dr. EL (Elinor) Scott, Prof. JH (Harry) Bitter
Group	:	Biobased Chemistry and Technology
Address	:	Bornse Weilanden 9 6708 WG Wageningen The Netherlands

WAGENINGEN
UNIVERSITY & RESEARCH

Abstract

A series of Pt-based activated carbon supported catalysts (Pt/AC) were prepared as potential catalysts for starch oxidation. The role of the surface chemistry (oxygen-groups) on the carbon support on the catalytic performance of Pt/AC catalyst for selective oxidation of carbohydrate was established. It is hypothesized, that the influence of the oxygen groups can be two-fold: First, during synthesis of the catalysts the presence of oxygen groups can enhance the dispersion of Pt on the support. Alternatively, the oxygen groups might influence the catalytic activity either by modifying the adsorption of the reactants or through an electronic effect on the Pt.

Different amounts of oxygen groups were introduced on the support surface by refluxing the carbons in HNO_3 for different times. The supports are characterized by N_2 physisorption and TPD-MS. It was demonstrated that depending on the severity of oxidation treatment, the surface area and the pore volume decreases. Moreover, it was shown that the amount of introduced oxygen groups are a function of the HNO3 concentration and the treatment time.

The Pt/AC catalyst with 5 wt.% loading and different oxygen-support densities were successfully synthesised with incipient wetness impregnation. The catalysts were either directly reduced or calcined at 250 °C before reduction in order to synthesises catalysts with a similar range of particle sizes. According to the chemisorption data, the calcined catalysts show smaller particles (1.6-1.8 nm) as the non-calcined catalysts (2.4-3.2 nm). The catalytic activity was determined by oxidizing glucose. The calcined Pt/AC catalyst with high oxygen density on the support shows the highest activity with a turnover frequency of 0.21 s^{-1}. These results show that the surface groups in combination with calcination enhance the glucose synthesis activity of the catalyst.

Contents

Introduction

1.1 Background

Over the last century the demand for renewable resources has grown rapidly due to the high utilization of fossil resources. Finding a substitute for fossil fuels is imperative because of our dependence on non-renewable sources. At the same time, it is challenging to find new resources and to simultaneously develop a green production process.

In this context, biomass is gaining attention as a class of renewable materials.[1] Biomass components, such as cellulose, lignin and starch, constitute a portfolio of many compounds which can be further converted into chemicals. Particularly starch is considered to be a promising raw material for the production of numerous high-value products since it is one of the abundant and inexpensive organic compounds in nature.[2-5]

From a chemical point of view, native starch is a polysaccharide and consists of two types of glucose polymers, the linear amylose and the branched amylopectin. Thickening agents, stabilizers, emulsifiers, fuel ethanol and bioplastics can be produced from native starch.[6, 7] However, the use of native starch is limited due to its fast thermal decomposition, insolubility and low shear stress resistance.[8] Therefore chemical modification of starch to improve its material properties would be favourable. The resulting starch would be more suitable for different applications. Examples of chemical modifications are oxidation, hydrolysis or esterification, which are effective methods to make starch more hydrophilic or hydrophobic.[8]

A common method yielding hydrophilic starch is to convert it into oxidized or anionic starch by selective oxidation. During this process a selective agent first oxidizes the hydroxyl groups (OH^-) to carbonyl groups and subsequently to carboxyl groups. The oxidation of starch can occur at two positions: either at the primary alcohol on the C6 atom or at the vicinal diols on the C2 and C3 atoms of the cellulose and amylose molecules leading to the cleavage of the bond (Scheme 1). Both reactions result in a carboxylic acid. Additionally, a partial depolymerisation also called degradation reaction takes place. Here the C1 carbon at the glucose chain end of the starch polymer is oxidized to COOH.

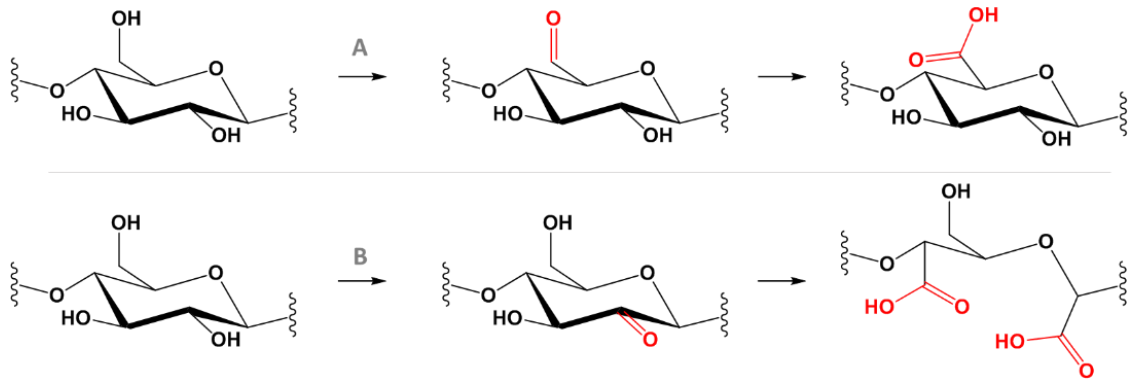

Scheme 1. Oxidation reactions of polysaccharides in two different ways: (A) primary alcohol oxidation on C6 and (B) oxidative cleavage between C2 and C3.

There are numerous food and non-food applications for oxidized starch.[2, 9] In particular, the paper, textile, laundry and binding materials industry are interested in oxidized starch because of its low viscosity, high stability, film forming and binding properties.[10] An example for an application is the replacement of polyacrylates and polyacrylamides which are superabsorbents widely used within the textile industry due to their good absorbing and retaining properties in large amounts of water. However, because of environmental concerns the use of those agents has been banned.[11] Oxidized starch was shown to be an efficient superabsorbent and is therefore considered to be a more environmentally friendly alternative.[12, 13]

The commercial oxidation of starch is well studied and highly efficient, but it carries environmental issues. The current production routes utilize hazardous bleaching agents, such as halogens and peroxides, yielding large quantities of inorganic toxic waste.[9, 10] Hence, alternative processes using hydrogen peroxide (H_2O_2) or oxygen as oxidant are to be preferred.[8] An oxidation method using hydrogen peroxide in combination with a copper sulphate catalyst has already been studied.[14, 15]

The use of homogenous catalysts was proposed for a greener production process of oxidized starch.[9, 16] Several homogeneous catalysts have already been developed, such as the TEMPO catalyst and the copper catalyst.[17] As a major drawback, systems employing homogenous catalysis are known for causing difficulties in separating the products from the catalyst during the downstream processing and in extracting and recycling the catalyst from the reaction medium.[18]

This study aims at employing a heterogeneous catalyst for the oxidation of starch, using air as a sustainable and environmentally friendly oxidant. Heterogeneous catalysts differ in their physical phase from the reactants and products which simplifies the separation process. To our knowledge, no heterogeneous catalysts for starch oxidation have been reported yet which might be due to the challenging, complex properties of starch. The oxidation of monosaccharides using heterogeneous catalysts, however, has been investigated.[19-21] High molecular weight carbohydrates such as starch show strong interactions with the catalyst and, therefore, may hamper the oxidation reaction, while low molecular weight carbohydrates exhibit less interaction with the catalyst. Additionally, monosaccharides are less affected by diffusion limitation due to their smaller molecular size.

In the present study, the selective oxidation of glucose as substrate with a heterogeneous catalyst is reported. The main products obtained by oxidation with air or hydrogen peroxide and a heterogeneous catalyst are gluconic, glucaric and 2-keto-fluconic acids (Scheme 2).[19] Gluconic acid is synthesized by oxidizing the hemiacetal hydroxyl in glucose to carboxyl. However, for the oxidation of starch, the heterogeneous catalyst should be able to oxidize the primary and secondary alcohols of glucose. Previous studies have shown that depending on the chosen metal; heterogeneous catalysts have the ability to oxidize glucose derivatives at the C-6 alcohol.[22-25] Vleeming et al. shows that methyl α-D-glucopyranoside can be oxidized to α-methyl glucuronic acid with platinum catalysts on carbon support.[25]

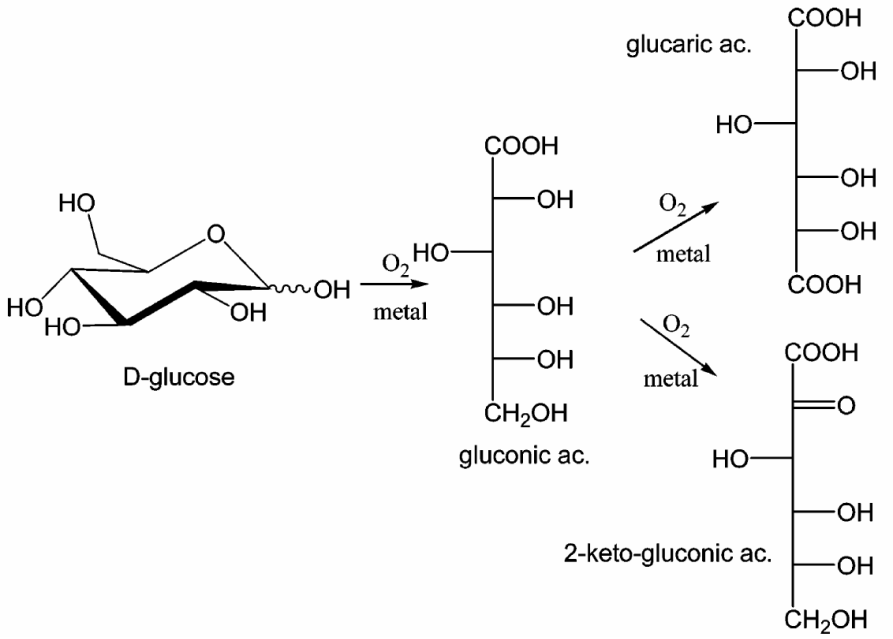

Scheme 2. Oxidation of glucose to gluconic, glucaric, and 2-keto-gluconic acids.[19]

1.2 Choice of heterogeneous catalyst

In addition to the substrate, the choice of the metal and support material is crucial. Platinum on activated carbon (Pt/AC) was shown to be suitable for the selective oxidation of carbohydrates (e.g. glucose) and was, therefore, chosen for this study.[26]

1.2.1 Metal

Metals, in particular gold (Au), platinum (Pt) and palladium (Pd) and their combinations, are known to exhibit both a high catalytic activity and a high selectivity towards the oxidation of sugars.[27-31] Also, catalysts with metal promoters, such as bismuth or lead, were synthesized to enhance the redox reaction of carbohydrate oxidations.[19]

A renewed interest in the monometallic Au catalyst has arisen due to its high conversion rate, selectivity and stability compared with Pt and Pd catalysts.[28, 32, 33] However, previous studies in this group have shown that gold catalysts on AC and on carbon nanofibers (CNF) only oxidize the reducing ends of the sugars, i.e., glucose, maltose and maltotriose.[34] Ultimately, the aim of this project is to oxidize starch, which would be inefficient using an Au catalyst since starch is a large polymer with only one reducing end.

Furthermore, an increased interest has been focused on supported platinum catalysts as an alternative to palladium or gold-based catalysts. Compared with the latter ones, platinum catalysts have higher redox potentials and are less prone to over-oxidation of the Pt surface.[35, 36] Delidovich et al. have shown that the glucose oxidation over a 5 wt.% Pt/AC catalyst exhibit a 30 times higher turnover frequency (TOF) for the gluconic acid production compared with that over a Pd/AC catalyst.[29]

1.2.2 Carbon supports

Carbonaceous materials have large specific surface areas and high porosities, durabilities and stabilities in aqueous solutions and in wide range of pH. This, together with their hydrophobic character, which is preferable to avoid interaction with the hydrophilic sugar molecules, make this material an attractive support for metal catalysts.[29, 37] Existing supports are active carbon (AC), carbon nanofibers (CNF), carbon black,[27] ordered mesoporous carbon and multi-walled carbon nanotubes.[38]

AC is the most widely studied carbon-based support for heterogeneous catalysts and has also been the material of choice for this study.[39, 40] The benefits of AC are its large surface area compared with other carbon materials and its commercial availability. In addition to its use as catalyst support, AC is used as an absorbent in water and gas treatment, in rubber production and for refractory materials.

AC is currently produced in two ways, either by chemical activation or by physical activation. During chemical activation, the carbons are simultaneously carbonized and activated at 600–800 °C with an activation agent such as phosphoric acid or zinc chloride.[41] Afterwards, the carbon is grained to obtain powder or granules. The most common raw materials for the production of AC are wood, coal lignite, coconut shell and peat. During this project, AC CA1 which is made from wood and SX Ultra which is made from peat are utilized as catalyst support.

Depending on the nature of the AC the structures and chemical surface areas differ. Therefore, AC is a very versatile material with tunable properties. This inhomogeneity of the material due to its variable nature hampers its usage as a standardized high-quality support.[42] Materials with different characteristics can be prepared using modification treatments to make them more homogenous.[43]

1.3 Support effect

The support has a strong effect on the catalytic performance including activity[44] and selectivity.[45] The carbohydrate oxidation rate is determined by two main factors related to the support. Firstly, the catalytic behaviour is determined by the (porous) structure which mainly affects the substrate diffusion during the reaction. Secondly, the surface chemistry of the support determines the carbon's hydrophilic or hydrophobic character and the metal's properties, e.g. its particle size and electronic effect.

The surface chemistry is dependent to a large extent by the foreign elements fixed to the surface, especially by oxygen.[46] Is has been established that there are several oxygen groups on the carbon surface, such as carboxylic acids, carbonyl, quinone, ether, phenol and lactone. Figure 1 presents the structures of oxygen groups on the carbon surface. The surface oxygen groups predominantly determine the support with respect to its acid/base and redox behaviour.[26, 40, 42] Thus, depending on the number and nature of the oxygen groups either a more hydrophilic or more hydrophobic carbon can be created. In general, it can be stated that the higher the oxygen content, the more acidic and therefore more hydrophilic the support is, whereas carbons with a low oxygen content have a more basic, i.e. hydrophobic, character.[46]

The concentration of the oxygen groups on the surface can be modified with oxidation agents. There are several treatment methods to introduce oxygen groups on the carbon surface: by gas-phase, liquid phase and by thermal treatment.[43] The liquid phase treatment is the most common one. Here, acid groups of are introduced by acids like nitric acid (NHO_3) or sulphuric acid (H_2SO_4).[46]

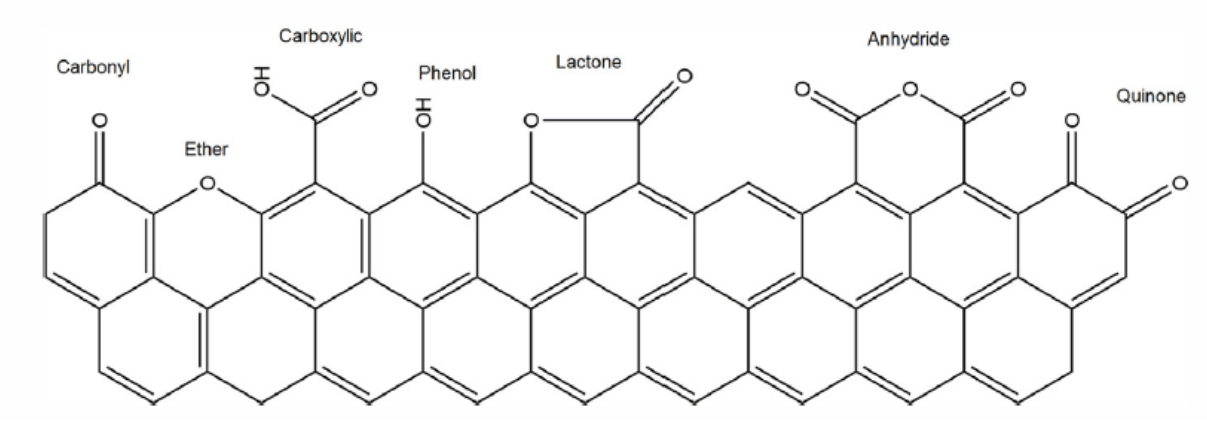

Figure 1. Surface oxygen groups on activated carbon.[43]

1.3.1 Effect of surface oxygen groups

The focus of this study is to investigate the effect of the surface oxygen groups on the catalytic performance of the Pt/AC catalyst for the selective oxidation of carbohydrates. It is hypothesized that the influence of the oxygen groups can be twofold. Firstly, during synthesis of the catalysts the presence of oxygen groups can enhance the dispersion of Pt on the support (Figure 2a).[26, 47] Secondly, the oxygen groups might influence the catalytic activity either by modifying the adsorption of the reactants or by an electronic effect on the Pt (Figure 2b).[26]

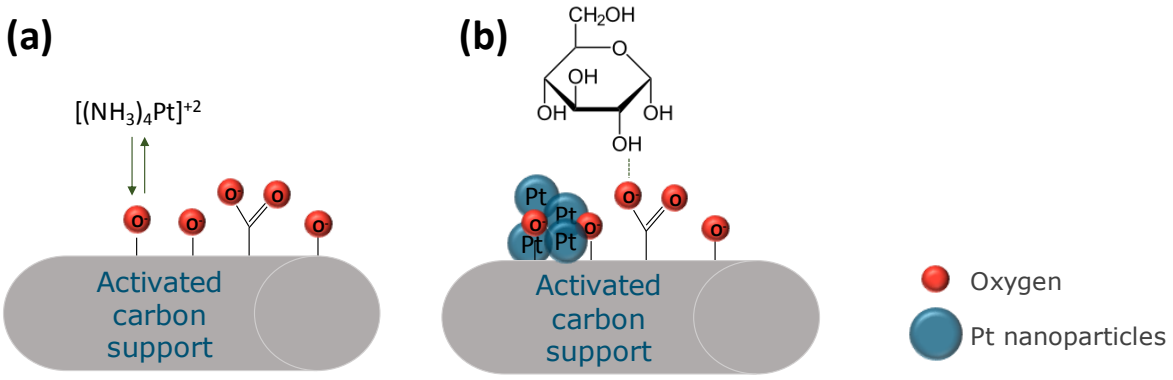

Figure 2. Schematic illustration of the support interactions, showing (a) the precursor-support interaction and (b) the substrate-support interaction.[48]

The metal dispersion and the particle size are fundamental characteristics of heterogeneous catalysts. The dispersion depends on the particle size or vice versa. The dispersion is used to gives an estimate of the metal atom availability for the catalytic reaction. It is also used to calculate the activity of the catalyst per surface metal atom, the TOF. The particle size provides an insight into geometric and

electronic influences on the catalytic performance.[26, 27, 49, 50] The geometric effect is based on the coordination number. Small nanoparticles have a lower coordination number and consequently offer more adsorption sites located on corners and edges adjacent to the substrate. In contrast, these reactive sites are severely reduced for larger particles and thus fewer sugar molecules can be transformed.[27, 34] The electronic effect consists of the change in energy level of the particle as it becomes smaller and is then also affected by the nature of the support. The support effect on the electronic effect depends on the surrounding functional groups. The amount of oxygen groups on the carbon surface changes the electronic state of the platinum due to electron donor/acceptor interactions. An oxygen-rich surface is expected to be higher in electron-rich platinum particle surfaces. As a result, the interaction between the platinum and the substrate changes and consequently the catalytic interaction is changed.

The particle size can be altered by introducing oxygen groups on the support's surface since surface oxygen groups form anchoring sites for metallic precursors and their metallic nanoparticles.[40, 47] During the synthesis, the loosely bound Pt particles will migrate on the support surface until they encounter Pt particles that are strongly bound to oxygen groups. In this way Pt particles enlarge until they reach a particle size which can be detected by Transmission electron microscopy (TEM) or chemisorption. Due to the fact that the formation of nucleation centers depends on the oxygen groups, the particle size will change with different amounts of oxygen groups present. Similar studies dealing with the effect of surface oxygen groups on the catalytic preparation and performance have been conducted. For example, Aksoylu and his co-workers modified the support of a Pt/CA catalyst to study the oxygen effect on the catalytic performance,[47] which was done by oxidizing AC with HNO_3 and comparing the resulting AC with a non-oxidized support. The results indicate that the modification has a significant effect on the support. The oxidation treatment enhances the dispersion of Pt on the AC support and leads to larger amounts of carboxylic acid groups.[47] Therefore, it can be deduced that the oxidation of the AC support also influences the catalytic performance.

1.4 Research objectives

The aim of this study is to alter the surface chemistry of the support to investigate the effect on the catalytic performance of a Pt/AC catalyst for selective oxidation. For this purpose the support surfaces will be modified by oxidation. The catalyst will be prepared with a Pt loading of 5 wt.%. Furthermore, the Pt/AC catalysis will be characterized in order to study the modification of the support and the Pt groups. The results will then be compared with the non-modified supported catalyst. To check the catalytic activity, a selective oxidation will be performed with glucose as substrate.

In this thesis the following research question should be answered:

"Which effect does the surface chemistry of the support has on the catalytic performance of Pt/AC in selective oxidation reactions?"

2 Experimental design

2.1 Research Approach

The research goal is to establish the role of support oxygen groups on the performance of platinum on activated carbon (Pt/AC) catalyst in selective glucose oxidation.

To investigate this, the research was divided into two stages. During the first stage, two different commercial ACs, SX Ultra and CA1 were compared based on their physical and chemical properties after the introduction of the oxygen groups on the surface by an acid treatment (Chapter 4). Based on this comparison, one support was chosen for the second stage of the research in which the catalytic performance was investigated (Chapter 5).

The two commercial AC (SX Ultra and CA1) were oxidized and used as support. The oxidation was done with various nitric acid (HNO_3) concentrations and treatment times. Subsequently, the effect of acid treatment on the carbon structure and surface chemistry in comparison to the non-treated carbon was investigated (Figure 3 A). This was done by TPD-MS, XPS, N_2 physisorption and TGA. Based on the TPD-MS decomposition spectra, the amount and type of introduced oxygen groups were investigated.

The 5 wt.% Pt catalysts supported on carbon were prepared by incipient wetness impregnation with $[Pt(NH_3)_4](NO_3)_2$ solution. Subsequently, the catalysts were either directly reduced at 300 °C or first calcined at 250 °C and then reduced (also at 300 °C), as an attempt to obtain similar particle sizes for catalyst prepared with oxidized and non-oxidized supports. Next, the dispersion and particle size was obtained by TEM, XRD and chemisorption characterization studies (Figure 3 B). Based on the results, an evaluation of the catalyst properties with AC surface oxygenated groups with the original AC was done. The catalytic performance of the synthesized heterogeneous catalysts was evaluated by the glucose oxidation in a batch reactor. The glucose oxidation was measured by titration of the formed acid and HPLC to determine the substrate and product concentration (Figure 3 C).

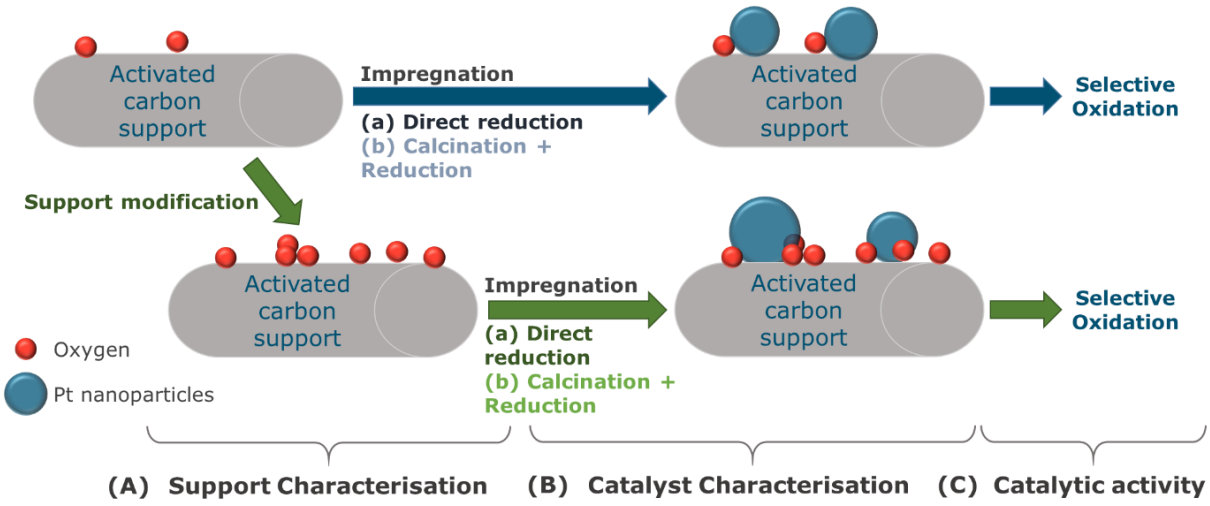

Figure 3. Overview of the procedure.

3 Material & Methods

3.1 Materials

The following chemicals are purchased from Sigma-Aldrich (DE): D-(+)-Glucose (≥99.5 %), D-Gluconic acid sodium salt (≥99 %), 5 wt.% Platinum on activated carbon, activated charcoal Norit CA1 from wood, Tertraannine Platinum (II) nitrate, (99.995 %), Chloroplatinic acid hexahydrate (≥99.9 %) and propionic acid (ACS reagent, ≥99.5 %). Activated carbon Norit SX Ultra was obtained from Cabot (US). The nitric acid (HNO_3, 68 %, technical grade) was purchased from VWR Chemicals (NL). Sulphuric acid (H_2SO_4, 98 %) was from Merck (NL). Potassium hydroxide (KOH) and sodium hydroxide (NaOH) were used from Fisher Scientific (UK).

3.2 Preparation and characterization of the AC support

3.2.1 Support preparation

Two commercial activated carbons (ACs), Norit SX Ultra and Norit CA1, were used as catalyst support. The ACs were either used as raw, washed (refluxed) or oxidized material.

For the refluxed form, 10 g of AC was refluxed with 200 mL of demineralized water for 1.5 h with the aim to remove water soluble impurities. This was followed by vacuum filtration and overnight drying at 60 °C. These washed samples are labelled “AC-refluxed”.

For introducing oxygen surface complexes on the supporter surface, the ACs were treated with different degrees of aqueous nitric acid ($HN0_3$) concentrations: 6.5 %, 12 % or 65 % (v/v) HNO_3 solution. The HNO_3 treatment was performed under reflux at boiling temperature for different durations. Table 1 gives an overview of the different sample preparations. Subsequently, the AC was vacuum filtrated and washed with approximately 2 L of demineralized water. The samples were dried overnight at 60 °C. All samples were labelled according to the following system: AC-ox. with the concentration percentages and refluxing time added as additional suffixes, e.g. “SX Ultra-ox. 6.5 % 1.5 h”.

All samples were weighted before and after the treatment in order to calculate the material loss.

Table 1. Summary of treatments conditions of the different prepared supports.

	HNO_3 Concentration	**Refluxing time**
SX Ultra	6.5 %	1.5 h
	6.5 %	3 h
	6.5 %	6 h
	12 %	0.5 h
	12 %	1.5 h
	12 %	3 h
	65 %	1.5 h
CA1	HNO_3 Concentration	Refluxing time
	6.5 %	1.5 h
	65 %	1.5 h

Physisorption

The surface area, total mesopore and micropore volume of all samples were derived through nitrogen (N_2) physisorption obtained with a Micromeritics ASAP 2020 from TriStar II PLUS (US). Prior to physisorption measurements, the samples were dried at 100 °C for ~1-2 h and degassed at 300 °C for 2 h. The degassing was performed in Micrometrics VacPrep 061 a Sample Degas System. For the calculations of the isotherm data plots, the BET (Brunauer–Emmett–Teller) method was used and the pressure region for fitting the linearized data was determined the Rouquerol method. For the pore volume and pore diameter, the BJH (Barrett-Joyner-Halenda) equation was applied to the desorption isotherm. The micropore volume was derived from the t-plot.

3.2.2 Temperature programmed desorption (TPD)

For the determination of the oxygen-bearing surface groups, TPD tests were performed on all supports. The analysis was performed in a Micromeritics AutoChem II *2920*. For this test, approximately 100 mg of sample was placed in the U-shaped tubular quartz reactor and introduced into the AutoChem instrument. Helium (He) was used as the carrier gas, and was applied with a flow rate of 50 mL/min He. The heating rate was set at 10 °C/min from room temperature to 900 °C. The obtained curves were analyzed with the software of micrometrics AutoChem II Chemisorption Analyzer.

The effluent gases were evaluated with the mass spectrometer THERMO^{StarTM} from Pfeiffer. The mass of CO/N_2 and CO_2 were evolved as a function of temperature and next to those gases, the O_2, H_2O He, H_2 and Ar were detected. The determination of the peak areas was calculated with MS Excel.

3.2.3 Thermogravimetric analysis (TGA)

Thermogravimetric data were obtained using a MultiSTAR® TGA/DSC sensors from Mettler Toledo, US. Depending on the samples, different measuring methods were used.

For the AC characterization, approximately 20 mg of AC was filled in aluminum cups and heated to 900 °C under inert conditions. For calcination analysis, the samples were either analyzed under air or nitrogen with a flow rate of 5 mL/min and 50 mL/min, respectively. About 5-10 mg of the precursor or catalyst was placed into alumina crucibles and heated up from 25 °C to 500 °C with a heating rate of 10 °C/min.

The TGA graphs were analyzed with the TA Universal Analysis software.

3.2.4 X-ray photoelectron spectroscopy (XPS)

XPS provides an estimation of the chemical surface composition of the few uppermost layers of the AC material. For all XPS analysis, a PS-9200 photoelectron spectrometer (Jeol, Japan) was used. The samples were measured by the Organic Chemistry Chairgroup of Wageningen University.

3.3 Catalyst preparation

The catalysts were synthesized through the incipient wetness impregnation technique. Initially, the pore volume of the different supporters was determined experimentally by adding Milli-Q water (MQ) until saturation of the ACs was reached.

A stock solution of the two precursors, tetraammineplatinum(II) nitrate ($[Pt(NH_3)_4](NO_3)_2$) and chloroplatinic acid hydrate ($H_2PtCl_6 \cdot xH_2O$), was made. To reach a Pt loading of 5 wt.%, the desired amount of precursors was dissolved in MQ corresponding to how the pore volume of AC support was determined.

1 g of the AC support was placed in a round bottom flask and the precursor solution was added dropwise to the AC support while shaking vigorously, until the support was saturated. After the impregnation, the catalyst was dried in the 60 °C oven overnight.

Some samples were calcined before the reduction to determine the influence on calcination on the oxidation reaction itself. For this, the catalysts were calcined for two hours at 250 °C in static air in a Nabertherm P 330 calcination oven with a heating ramp of 5 °C/min. The calcination temperature was optimized by studying the precursor degradation (see Appendix I).

For the reduction, the catalyst was placed in a tubular quartz reactor and reduced at 30 % H_2 and 26 % N_2 atmosphere from full scale of 100 mL/min. The catalyst was heated with a temperature ramp of 5 °C/min up to 200 °C, at which it was kept for 2 h. During cooling down (~30 min) the catalyst was kept under the gas flows. These were followed by a 30 min N_2 flushing.

3.4 Catalyst Characterization

3.4.1 X-ray Diffraction (XRD)

The XRD patterns were recorded on a Bruker D8 Advance with an Lynxeye-XE-T PSD detector to get an insight of the crystalline structure and the Pt particle size. Approximately 200 mg of each sample was brought into a PMMA round sample holder and introduced into the XRD. The samples were scanned in Bragg-Brentano geometry from 10° to 80° 2-Theta at room temperature using a step size of 0.05° at 1 second per step, with fixed sample illumination (20 mm), automatic anti air-scatter screen and 2.5° primary and secondary axial soller slit. The platinum particle (crystallite) size was estimated by Rietveld refinement using TOPAS using the fundamental parameter approach. The contribution of the support was first determined by modelling the diffraction patterns of the pure support materials by a Pawley type fit using 2 arbitrary unit cells (hexagonal (P63mc) and orthorhombic (Fmmm)) for the carbon contributions and the quartz (trigonal (P3121)) from the Crystallography Open Database (COD). Scaled contributions of the support were then using for fitting the catalyst together with the refinement of the platinum and quartz contributions.

3.4.2 Chemisorption

3.4.2.1 Pulse chemisorption

Pulse CO or H_2 chemisorption was performed on a Micromeritics AutoChem II, Chemisorption Analyzer. The measurements were either carried out in CO or in H_2 gas. For the measurements, about 200 mg of catalyst was placed in the Analyzer. The catalyst was reduced from room temperature to 150 °C with a temperate ramp of 10 °C/min in a helium for CO or argon atmosphere. The temperature was kept constant for 90 min, where the sample was reduced. Afterwards, the sample was cooled down to 35 °C. Pulses of CO or H_2 were injected.

The dispersion of metal particles in the catalysts was studied under the assumption of CO:Pt = 1:1 and H_2:Pt = 1:2 stoichiometry.

3.4.2.2 Static chemisorption

The static chemisorption was performed on a Micromeritics ASAP 2020c. Around 40 mg of the sample was placed in an alumina TGA crucible inside the quartz flow thru tube. The pretreatment protocol consist of three reduction at 100 °C, 110 °C and 300 °C in static hydrogen and subsequently two evacuation for 120 min at 300 °C and 10 min at 35 °C. Before starting the measurement an leaking test was done in which the maximum allowed outgas rate was set to 13 µmHg/min.

The first isotherm consist of the total gas uptake. After taking the first, an evacuation was done and the second isotherm was measured. The monolayer uptake was obtained for a linear fit of the isotherm in the pressure region of 150-600 mbar. The dispersion and particles size were calculated from the monolayer uptake using the known Pt loading and sample mass assuming a H2:Pt stoichiometry of 1:2.

3.4.3 Transmission electron microscope (TEM)

To visualize the Pt nanoparticle distribution over the carbon support and the mean diameter of the Pt nanoparticles, the catalyst was examined by TEM. The TEM images were obtained using a JEOL JEM-1011 Electron Microscope. Samples were prepared by dispersion in 99.9% methanol and sonicating them for 30 min in the ultrasonic bath. Some drops (2 µL) of the sample suspension was then deposited on a commercial carbon-coated copper grid and dried by using a piece of filter paper at room temperature. Particles size distribution were obtained by counting 300-400 particles with ImageJ software.

3.5 Heterogeneous oxidation reaction

The activity of the synthesized catalysts Pt on AC was investigated by an oxidation reaction with the substrate as D-(+)-glucose. The are two used oxidation set up, referred to as heterogeneous oxidation set up 1 and 2. The commercial Pt/AC catalyst with a metal loading rate of 5 wt.%, was used for optimization of the oxidation conditions for the reactor set up 2 (Appendix II). The oxidation of glucose was used as a model reaction since all catalysts oxidize this substrate.

All oxidation reactions done with AC Norit CA1 as support material were performed at the same condition used by my predecessor.[22] The following conditions were applied: a temperature of 50 °C, a substrate concentration of 0.1 M dissolved in 50 mL of demineralized water, a O_2-flow rate of 300 mL/min, a substrate: metal ratio of 900 mole/mole and the pH 9 was kept constant by adding 0.5 M NaOH solution with the help of pH stat Ω Metrohm 800 Dosino3. As reactor, a three-necked 100 mL round bottom flask was used, which was connected to the base pump and the pH electrometer. The reaction mixture was heated using an oil bath on a hot plate. In Figure 4 the reaction set up 1 can be seen.

Figure 4. Heterogeneous oxidation set up 1 for the reactions conducted with catalyst supported on AC.

The oxidation reaction with the AC Norit SX Ultra as support was carried out in the a three-necked jacketed glass reactor vessel equipped with a pump for alkali supply and combined electrode for the pH registration. The heterogeneous oxidation set up 2 can be seen in Figure 5. 250 mL of demineralized water was heated up using a heating water pump and stirred at 2000 rpm with a head stirrer. The pH was adjusted to 9 and kept constant with pH stat Ω Metrohm 800 Dosino3 with a 0.5 M NaOH solution. The O_2-flow was 300 mL/min and the substrate: metal ratio was 447 mole/mole with a 0.05 M substrate concentration.

During the oxidation, 500 µL samples for analysis were periodically drawn from the reaction mixture (0 min, 5 min, 10 min, 15 min, 20 min, 30 min, 45 min, 60 min and 120 min). After the oxidation, the catalyst was recovered from the reaction medium through vacuum filtration, washed with about 0.5 L demineralized water, and dried overnight at 60 °C.

Figure 5. Heterogeneous oxidation set up 2 for the reactions conducted with catalyst supported on AC.

3.6 High-Performance Liquid Chromatography (HPLC) analyses of oxidation samples

The performance of the catalyst was evaluated by substrate (glucose) and product (gluconic acid) identification, and quantification using Dionex UltiMate 3000 RS autosampler HPLC on an Aminex HPX-87H, 300x7.8 mm (BioRad 125-0140) column at 35 ^{o}C.

The samples of the reaction mixture were thoroughly filtered to remove the catalyst by a 1 mL Terumo® syringes in combination with a Phenomenex RC membrane 0.2 µ filter. 300 µL of the filtrate was diluted in the internal standard solution 250 mM propionic acid in 1 M H_2SO_4 with a 1:1 ratio. Calibration curves of the substrate and the main product were taken into each measurement, with concentrations of 25, 5, 2.5 and 0.5 g/L. As mobile phase, 5 mM H_2SO_4 with a flow of 0.5 mL/min was used and a detection wavelength of 210 nm.

3.6.1 Oxidation performance

The oxidation performance represented by the glucose conversion and selectivity and gluconic acid yield was calculated by the following equations;

$$\text{Conversion} = \frac{[\text{sustrate}]_{\text{inital}} * [\text{substrate}]_{\text{t}}}{[substrate]_{initial}} * 100\ \% \qquad \text{(Eq. 1)}$$

with $[substrate]_{inital}$ being the respective initial substrate concentration and $[substrate]_t$ the substrate concentration at time point t

$$\text{Selectivity} = \frac{[\text{product}]_{\text{t}}}{[substrate]_{initial} - [substrate]_t} * 100\ \% \qquad \text{(Eq. 2)}$$

with $[product]_t$ being the respective initial substrate concentration at time point t

$$\text{Yield} = \frac{[product]_t}{[substrte]_{initial}} * 100\ \% \qquad \text{(Eq. 3)}$$

3.6.2 Catalytic activity

In order to evaluate the catalytic performance the turnover frequency (TOF) for the gluconic acid production via selective oxidation of glucose for all catalyst was calculated. For that the TOF was determined by the HPCL data after reaching a gluconic acid yield of 10 %.

$$TOF = \frac{\text{n}_{\text{product}}}{D_{Pt} * n_{surface\ metatl} * t} \qquad \text{(Eq. 4)}$$

with $n_{product}$ being the respective amounts of gluconic acid moles present in the reactor after reaching a yield of 10 %, D_{Pt} being the dispersion obtained by the static chemisorption, $n_{surface\ metal}$ being the amount of Pt moles present in the reactor and t for time after reaching 10 % yield.

Next to this, the initial TOF (TOF_i) was calculated. That is done by calculation the initial reaction rate of the gluconic acid production.

$$Reaction\ Rate\ (R) = \frac{n_{product}}{V * t} \qquad \text{(Eq. 5)}$$

with V being the volume of the reactor mixture and t for time at taking the sample.

$$TOF_i = \frac{R * V}{n_{surface\ metal} * D_{Pt}} \qquad \text{(Eq. 6)}$$

4 Results & Discussion 1

4.1 Comparative study of the support oxygen group introduction on Norit CA1 and Norit SX Ultra

In this chapter two activate carbons (ACs), Norit CA1 and Norit SX Ultra, are compared. The pristine and the oxidized ACs were analyzed and characterized by different methods, namely physisorption, XPS and TPD. Different nitric acid (HNO_3) concentrations and treatment durations were applied and their effect on the AC support was investigated. The treatment with 6.5 % and 65 % (v/v) nitric acid (HNO_3) concentration and both with a 1.5 h refluxing time are compared. The synthesized Pt/AC catalysts were characterized by glucose oxidation, chemisorption and XRD. Only the results of the catalyst prepared on CA1 are shown during this section.

Based on the results and analysis of the different characterization measurements, it was concluded to continue with the SX Ultra as AC support for the catalyze synthesis. The catalyst characterization and oxidation results of SX Ultra are shown in chapter 3.

4.2 Weight loss during the HNO_3 treatment

The functionalization of the AC was implemented with HNO_3 treatment to create oxygenated groups on the surface. The carbon weight was measured before and after the treatment to calculate the material loss during the HNO_3 treatment (Table 1). Before recovering the material, it was left to settle down overnight. The weight of the 6.5 % oxidized ACs slightly decreases (5 %) which can be explained due to experimental loss. Both carbons treated with 65 % (v/v) show a higher material loss up to 46.1 % for the CA1 and 5.0 % for the SX Ultra. This loss indicates that the highly concentrated HNO_3 leads to disintegration of the material.

Table 1. Summary of the weight loss during the HNO_3 treatment.

Sample Name	Weight before (g)	Recovered Yield (g)	Weight loss (%)
CA1-ox. 6.5 % 1.5 h[a]	10.1	9.6	5.0
CA1-ox. 65 % 1.5 h[b]	9.9	5.3	46.1
SX Ultra-ox. 6.5 % 1.5 h[a]	10.0	9.5	5.0
SX Ultra-ox. 65 % 1.5 h[b]	10.0	7.6	19.4

[a] AC oxidized by 6.5 % (v/v) HNO_3 for 1.5 h [b] AC oxidized by 65 % (v/v) HNO_3 for 1.5 h

4.3 Physical characterization of the activated carbon supports

The textural properties of all ACs supports are investigated by nitrogen (N_2) adsorption, a widely known method to determine the surface area and the pore size distribution of solid materials. The adsorption/desorption isotherms of the CA1 are shown in Figure 6 and the one of SX Ultra in Figure 2. The textural parameters of all the carbon, calculated from the N_2 physisorption experiments are summarized in Table 2.

Table 2. Textural properties of different activated carbons. All calculated values from this table result from one measurement. '–' means that values are too small to be shown.

Samples	BET surface area in m^2/g	Total pore volume in cm^3/g	Micropore volume in cm^3/g	Mesopore volume in cm^3/g
CA1[a]	1016	0.79	0.24	0.58
CA1-ox. 6.5 % 1.5 h[b]	423	0.29	0.11	0.19
CA1-ox. 65 % 1.5 h[c]	< 1	-	-	-
CA1-reflux	1150	0.88	0.24	0.65
SX Ultra[a]	789	0.51	0.20	0.43
SX Ultra-ox. 6.5 %-1.5 h[b]	762	0.49	0.20	0.25
SX Ultra-ox. 65 % 1.5 h[c]	4	-	-	-
SX Ultra-reflux	662	0.42	0.18	0.33

[a] Original AC [b] AC oxidized by 6.5 % (v/v) HNO_3 for 1.5 h [c] AC oxidized by 65 % (v/v) HNO_3 for 1.5 h

Analysing the adsorption/desorption isotherms of the carbons with the IUPAC classification, the profile can be described as a combination of type I and IV.[51-53] The IUPAC type I isotherm is characteristic of micropore adsorption at low partial pressure, while the mesopores exhibit type IV behaviour in the IUPAC classification.[53] Type IV curves typically show the shape of a hysteresis loop emerged due to capillary condensation which commonly happens in mesoporous structures at a higher partial pressure. In Figure 6, showing the original CA1, a hysteresis loop can be seen between the adsorption and the desorption. That indicates that the CA1 consist mainly of a mesoporous structure. For the 6.5 % HNO_3 treated carbon the hysteresis loops become thinner and shift to a lower relative pressure (P/P_0) (Figure 6). There is almost no hysteresis loop for the 65 % HNO_3 treated carbon and also the type I isotherm characteristic are not clearly distinguishable (Figure 6). Therefore, it is suggested that the HNO_3 treatment leads to a reduction of the mesopore structure. This is also expressed by the calculated mesoporous volume in Table 2. The surface area and pore volume of the original CA1 are 1016 m^2/g and 0.79 cm^3/g, respectively. The surface area and the total pore volume of the AC treated by HNO_3 were reduced with increasing HNO_3 concentrations. The CA1 6.5 % was reduced by 58 % and for the 65 % treated carbon, no surface remains after the harsh treatment. Therefore, the values of the BET surface area in Table 2 are negative, and the pore volumes are not calculated. The significant decrease in surface area and pore volume can be explained by the collapse of the pore walls due to a high HNO_3 concentration during the oxidation.[47]

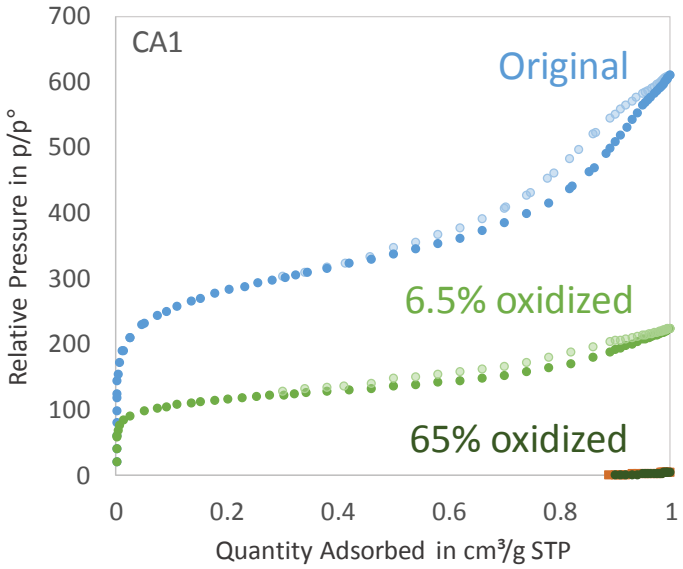

Figure 6. Adsorption/desorption isotherm profiles taken by N_2 physisorption of original AC CA1, AC CA1-ox. 6.5 % 1.5 h and AC CA1-ox. 65 % 1.5 h support materials.

The N2-physisorption isotherms for SX ultra, shown in Figure 7, shows a similar pattern as the CA1 one. The pristine carbon has a lower BET surface area (789 m^2/g) and a total pore volume (0.51 cm^3/g) compared to the CA1. Both IUPAC types I and IV with the hysteresis loops can be recognized in the isotherm profiles of the original and 6.5 % HNO_3 treated carbon. Noticeable is the fact, that the 6.5 % HNO_3 treated support does not show a decrease in surface area and pore volume (Table 2 and Figure 7), whereas the CA1, treated with the same concentration, does decrease in area and pore volume. The 65 % HNO_3 oxidation leads to a significant decrease in the area and pore volume due to the attack of highly concentrated HNO_3 similar to the CA1 one. Therefore, the SX Ultra has a lower BET surface area, however, it is expected to be more stable towards HNO_3 treatment.

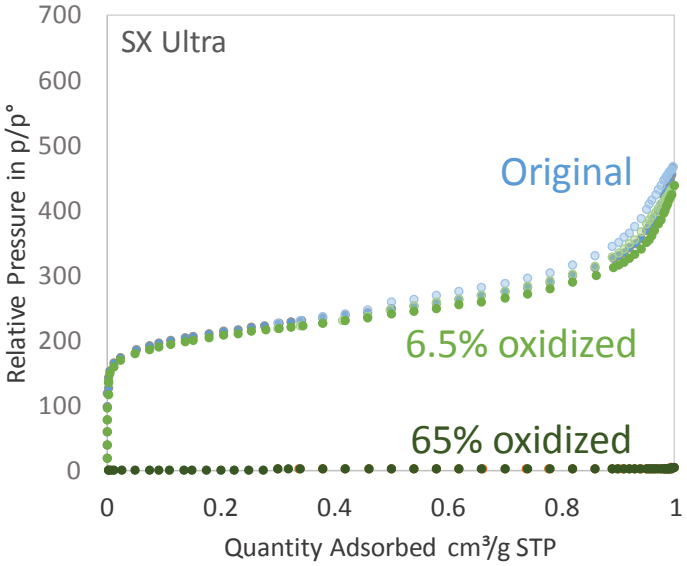

Figure 7. Adsorption/desorption isotherm profiles taken by N_2 physisorption of original AC SX Ultra, AC SX Ultra-ox. 6.5 % 1.5 h and AC SX Ultra-ox. 65 % 1.5 h support materials.

The pore size distribution of the materials is given in Figure 8. The largest pore volume of the pristine CA1 was in a pore size range of 10 nm. Due to the HNO_3 treatment, the pore volume of CA1-ox. 6.5 % 1.5 h shifted towards a small pore size less than 10 nm. The pore size distribution of original SX Ultra, as well as the HNO_3 treated one depicted in Figure 7, indicate that the largest pore volume was contributed by small pore size. For all carbons, a large peak at approximately 5 nm can be observed. This is an artefact peak and can be neglected.[54] The pore size distribution of the 65 % treated carbons are not shown due to the low micro- and mesopore volume after the acid treatment.

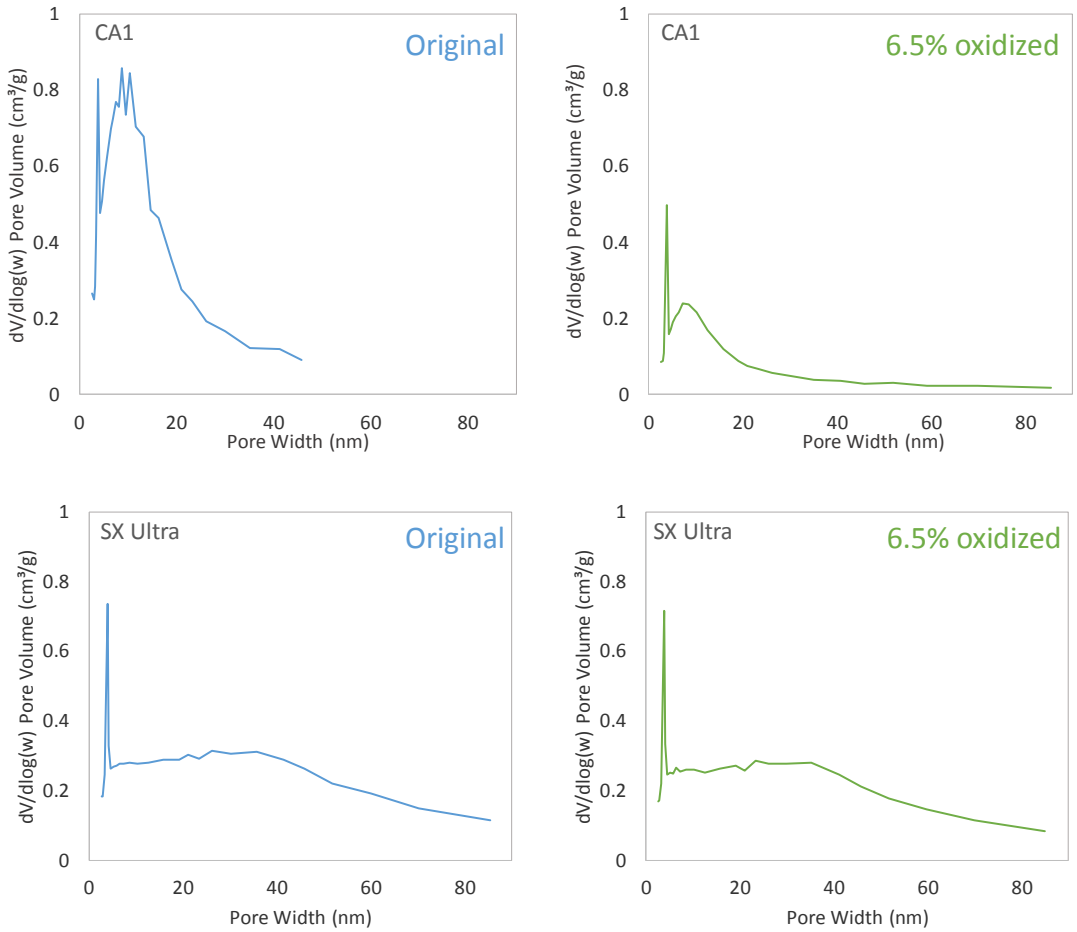

Figure 8. Differential pore size distribution taken by N_2 physisorption of original AC CA1 and SX Ultra and AC CA1-ox. 6.5 % and SX Ultra-ox. 6.5 %. Pore width represents in 1 nm = 10 Å.

The textural parameters AC-refluxed were measured to investigate the effect of the refluxing and heating treatment on the support area and pore volume. The samples were refluxed in water instead of an HNO_3 solution. As expected, the supports do not show any significant variation in their BET surface area or total pore volume, as can be seen in Table 2.

Consequently, it can be said that the SX Ultra has a much more stable physical structure after the oxidation treatments compared to the CA1. The SX Ultra does not significantly change the physical properties, after the acid treatment. The different AC stabilities toward the HNO_3 treatment can be explained by different origin in nature of the CA1 and SX Ultra.

4.4 Surface characterization of the activated carbon supports

The surface chemistry of the supports was analyzed by different techniques, such as XPS and TPD. Respective results will be discussed individually. Next to that, TGA measurements are done which are shown in Appendix III.

4.4.1 XPS

Characterisation with XPS was performed to analyze the surface atoms of the support, which results are shown in Table 3. Only the oxidized supports of CA1 are measured with this technique. The wide scans and narrows scans of the of the oxygen peaks are measured and can be found in the Appendix III.

From Table 3 it can be seen, that the main carbons peaks are located at the position 284-283 eV. The oxygen peaks are observed at binding energies of 530 and 531 eV. By comparing the two pristine AC, the CA1 has a higher original oxygen content. Due to the surface oxidation process, the CA1-ox. samples contain a higher surface oxygen percentage compared to the original carbon. For the 6.5 %, the oxygen percentage increases from 10.5 % to 19.0 % and for the 65 % treated CA1 the oxygen contribution increases to 28.0 %. From these results, it is demonstrated that the oxidation process can increase the density of the oxygen group on the support surface and the amount of oxygen increase with increasing HNO_3 concentration. This shows that the HNO_3 concentration can be used to control the amount of oxygen groups introduced to the AC.

Table 3. XPS results from different activated carbons.

Samples	Carbon		Oxygen	
	%	Binding Energy in E/eV	%	Binding Energy in E/eV
CA1[a]	89.5	283	10.5	531
CA1-ox. 6.5 % 1.5 h[b]	79.0	283	19.0	531
CA1-ox. 65 % 1.5 h[c]	68.8	284	28.0	531
SX Ultra[a]	94.4	282	5.6	531

[a] Original AC [b] AC oxidized by 6.5 % (v/v) HNO_3 for 1.5 h [c] AC oxidized by 65 % (v/v) HNO_3 for 1.5 h

4.4.2 TPD Characterisation

Studying the decomposition of the oxygen-containing groups on carbon surfaces into CO and CO_2 is a well-established method in literature.[55-58] It is a technique were specific oxygen groups are released by heating up the sample. The TPD profiles give an estimation of the amount of introduced oxygen groups on the support surface during the HNO_3 treatment.

From the TPD profiles of the CA1, presented in Figure 9, it can be seen that the TPD signal drastically increases after HNO_3 treatment. That is indicated by the peaks at the temperature range of 300-400 °C, which cannot be observed for the non-oxidized and refluxed carbon samples. It is expected that the peaks are a consequence of the oxygen groups introduced on the support, which is confirmed by the MS data. By introducing oxygen groups on the support surface, the hydrophobicity of the AC changed. From literature, it is known that increasing hydrophilicity of the support promotes the deposition of

the metal.[26] Therefore, a higher oxygen content on the carbon support is profitable for the catalyst synthesis.

All CA1 carbons show a peak at around 100 °C, which do not belong to the release of CO and CO_2. The MS data given in the Appendix V indicate that this peak can be attributed to water.

From the XPS data is known, that the original CA1 contains 10 % oxygen surface atoms. However, the TPD results for the original CA1 show an extreme drift below the baseline at 300-400 °C at which the release of oxygen groups was expected. By looking for an explanation of this negative drift, TPD and MS measurements with no sample and only glass wool were taken to study the "background" signal of these measurements (Appendix VI). Although a slight drift below the baseline can be identified for the TPD data, there is no explanation for the drastic drift of the CA1 samples. Also the MS results show no significant differences. Consequently, no reasonable explanation for the negative drift could be found yet.

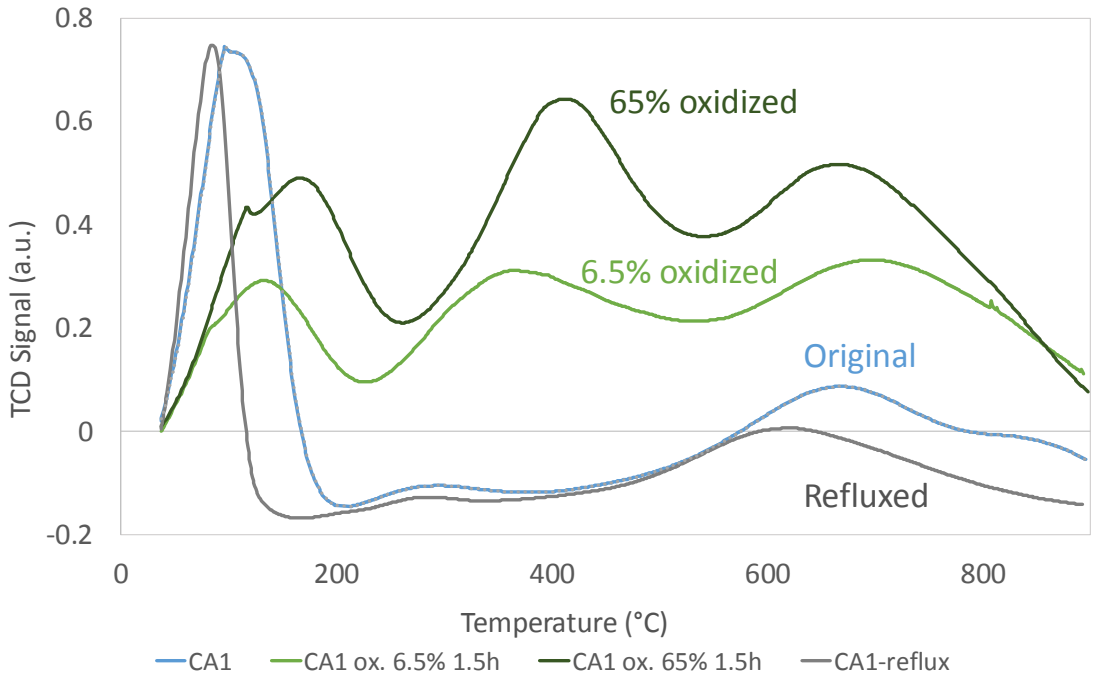

Figure 9. TPD profiles in He with 10 °C/min for **CA1** before and after HNO_3 treatment.

The SX Ultra TPD profile in Figure 10 shows similar results to those found for the CA1: an oxidation treatment leads to an increasing TPD signal. However, the intensity of the TPD signal is in total lower compared to that of CA1. While 6.5 % oxygen treated CA1 shows a drastic increase at 300-500 °C, the SX Ultra-ox. 6.5 % merely increases slightly. Next to that, the spectra show a similar drift as it was noted for the CA1 and CA1-reflux. The intensity of the TPD signal from the oxidized SX Ultra is in general lower compared to the one of CA1. From that, it can be concluded that the amount of introduced oxygen groups is lower compared to the CA1 treated under the same conditions. As the XPS results already show, the CA1 is richer in oxygen-bearing surface groups than the SX Ultra, which is confirmed by the TPD data.

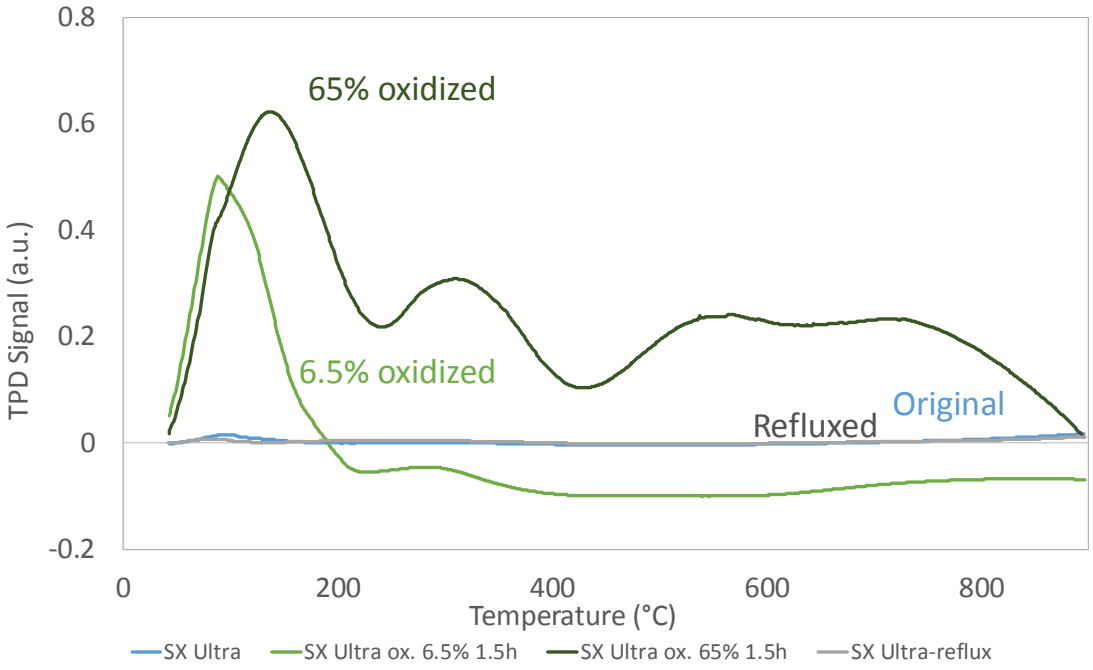

Figure 10. TPD profiles in He with 10 °C/min for **SX Ultra** before and after HNO_3 treatment

During the TPD, the oxygen-containing chemical groups are decomposed to CO and CO_2. The decomposition was investigated by analyzing the effluent gases with MS. There is a lot of discussion regarding to the decomposition of a specific surface group in literature. The decomposing is affected by many variables such as physical properties of the material or the heating rate.[59, 60] However, some general trends have been established. Figueiredo et al. set up a decomposition ranking of specific oxygen groups as can be seen in Figure 11.[60, 61] It is stated that the carboxylic acids decompose to CO_2 at 100-450 °C, anhydrides decompose into CO and CO_2 at 350-600 °C, lactones release CO_2 at higher temperatures like 550–800 °C, phenols release CO at 500-750 °C and carbonyl and quinones decompose by releasing CO at 650-900 °C.[62] Thus, CO_2 is released at low temperatures, while the decomposition of CO peaks can be found in a higher temperature range. This trend for the CO and CO_2 decomposition can be seen back in the MS data of CA1 and SX Ultra (Figure 12 & Figure 13).

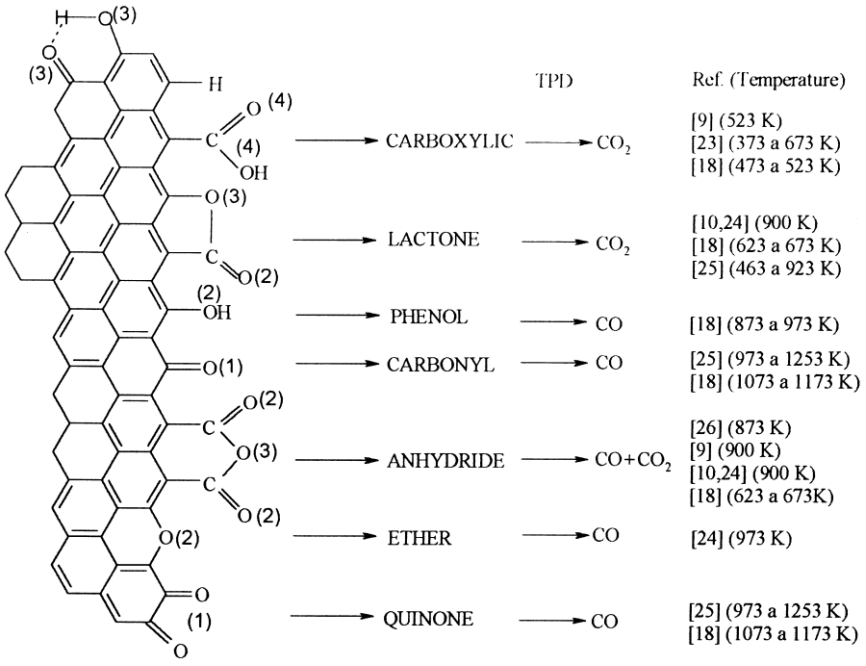

Figure 11. Surface groups on carbon and their decomposition by TPD.[60]

The MS spectra under helium (He) were obtained for all carbon supports. The CO and CO_2 profiles of CA1 and SX Ultra are similar. The shifts on the ion current scale of the peaks result from the use of the SEM (CA1 has a maximum of 1.5E-9 while CA1-ox. 6.5 % ends at 4.0E-11). The SEM detector is more ion-sensitive and effectively multiplying the single incident ion by 10^6 or more.[63] The graphs are shown to give an insight of the decomposition profile of the CO and CO_2 during the TPD measurements. Since only a CO and CO_2 calibration was done with the SEM detector, a comparable quantification of CO and CO_2 release was not conducted.

A comparative analysis shows that the samples oxidized with HNO_3, have the highest amount of oxygen-containing surface groups. That is in line with the TPD and XPS data. Both pristine carbons, CA1 and SX ultra, have a low CO_2 release, while for the acid treated carbons the CO_2 decomposition significantly increases. That indicates that mainly carboxylic acids (and anhydrides) are introduced during the HNO_3 treatment, originating a support with acidic and hydrophilic characteristics.[59] The original carbons show a small CO decomposition, which mainly results from pyrolysis. Whereas, after the HNO_3 treatment, the CO decomposition increases. It is proposed that the increase of CO results from the introduced anhydrides and lactones.[47]

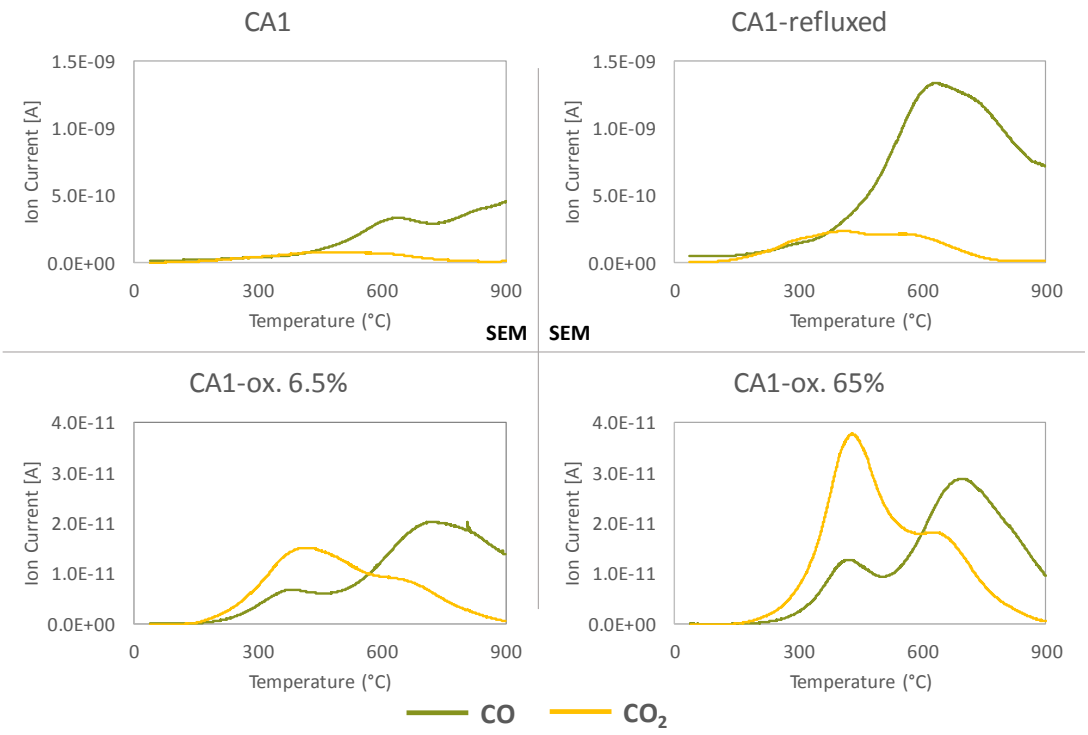

Figure 12. MS spectra of different AC **CA1** before and after oxidation treatment. The graphs highlighted with SEM indicates that the measurements are taken with a secondary EM detector.

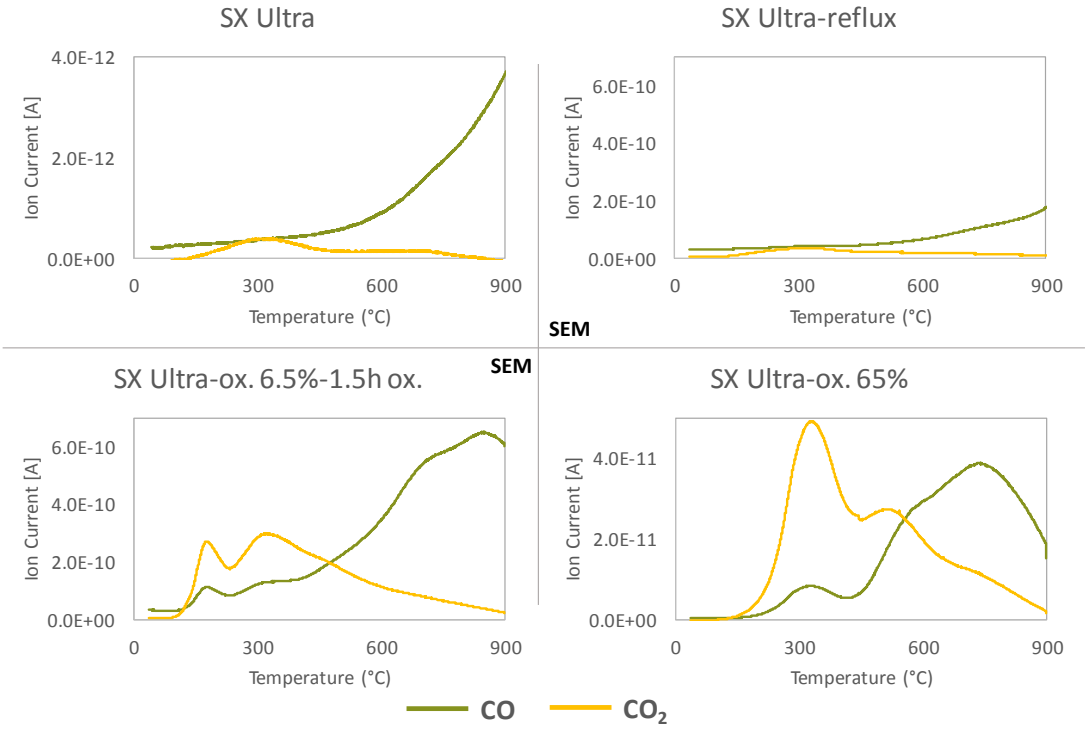

Figure 13. MS spectra of different AC **SX Ultra** before and after oxidation treatment. The graphs highlighted with SEM indicates that the measurements are taken with a secondary EM detector.

In summary, the thermal treatment is a powerful technique to study the modified surface chemistry of the AC and leads to a selective removing of the specific oxygen groups. From the above shown TPD results, it could be seen that CA1 introduce more specific oxygen groups to its surface compared to the SX Ultra.

4.4.3 Conclusion on comparison

During this chapter, both possible carbon support, CA1 and SX Ultra treated with HNO_3 were characterized by physisorption, XPS and TPD to study. The aim was to increase the oxygen density on the support without changing the textural properties. The results of the experiments carried out of the of the oxidized support and non-oxidized support of CA1 and SX Ultra indicated that (i) the textural properties of the AC decreases with higher HNO_3 concentration, especially for the CA1 and (ii) that the HNO_3 oxidation leads to the formation of surface oxygen bearing groups which decompose to CO and CO_2 at higher temperatures, for both supports.

In order to optimize this acid treatment to compose a carbon with a high oxygen density and same textural properties, the treatment time as a new variable can be taken into account.

4.5 Glucose oxidation with CA1 supported catalyst

For further experiments, the CA1 was chosen based on the following reasons: (i) the TPD data highlighted that more specific oxygen groups are introduced at the CA1 surface compared to SX Ultra and (ii) previous work has shown that the SX Ultra is contaminated by silica (quartz). It is assumed that the silica does not have a significant effect on the catalyst preparation or performance. However, it hampered the XRD characterization of the catalyst, since the platinum and silica have some overlapping peaks in the XRD pattern. For this reason, initially, the CA1 was chosen as support.

To evaluate the catalytic performance, the glucose oxidation was conducted using three different catalysts i.e. Pt/AC, Pt/AC-ox. 6.5 % 1.5 h and the Pt/AC-refluxed in the liquid phase oxidation under standard conditions of the heterogeneous oxidation set up 1 (Section 3.5). The results of the oxidation, shown by the acid formation from three different catalysts are presented in Figure 14. The chemical functionalization resulting in the formation of oxygenated surfaces, leads to a decreased catalytic activity (green), whereas the catalyst with a non-treated support and with refluxed support show a similar trend and a higher oxidation rate. It seems that higher amounts of oxygen groups on AC support have a negative effect on the selective oxidation glucose.

To conclude, it should be stressed that catalyst prepared with an oxidized CA1 support do show no catalytic activity, while the catalyst prepared on the original CA1 do show activity. This decrease in activity is going to be investigated in the following section.

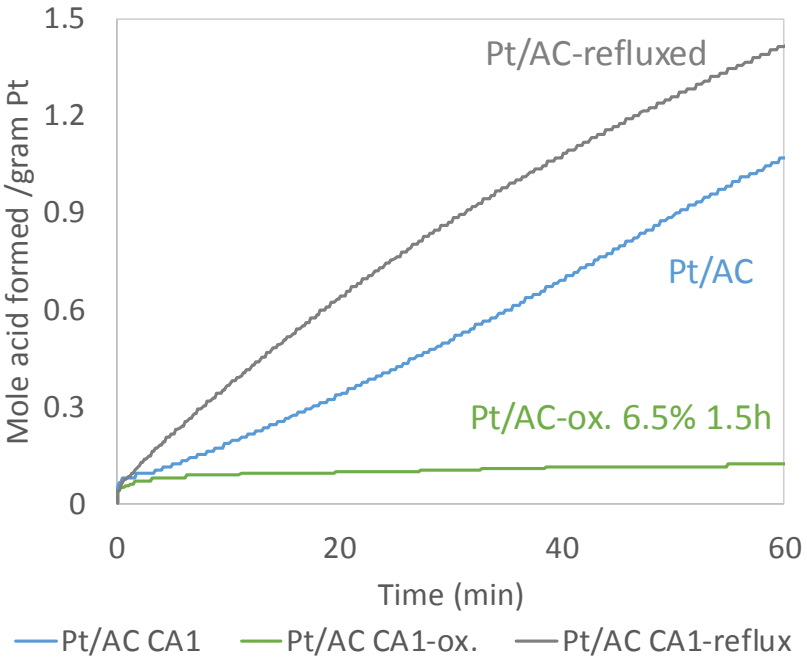

Figure 14. The catalytic activity of different platinum catalyst with different AC **CA1** supporters. Reaction performed at 50 °C, pH =9, 0,1M substrate concentration, substrate: metal ratio of 900 mole/mole and oxygen flowrate = 300 mL/min.

4.6 Catalyst characterization

The significant decrease in activity of the catalyst with oxidized support can be caused by many reasons: due to adsorption of the substrate, electronic effect of the support or particle size effect. To get an indication of the particles size, the catalysts were analyzed with XRD from 10° to 80° 2-Theta. Due to the high metal loading (5 wt.%) (and no contamination of the silica), the platinum could be clear visualized in the XRD pattern in Figure 15. The diffraction peaks at (111), (200), (220) and (311) at 39.8° 2-Theta, 46.2°, 67.5° and 81.3° 2-Theta are ascribed to metallic platinum.[49, 64] According to the XRD results, the catalysts with low an oxygen content on the support have relatively large particles, referring to the lager peaks at 40° and 70° 2-Thera. For Pt/AC–ox. no clear peaks at 40° 2-Theta are visible and by comparing the catalyst with the support AC-ox. (dark blue), it shows a similar pattern. That indicates that either a low amount of Pt particles is attached or very small Pt particles are presence on supported on carbon.

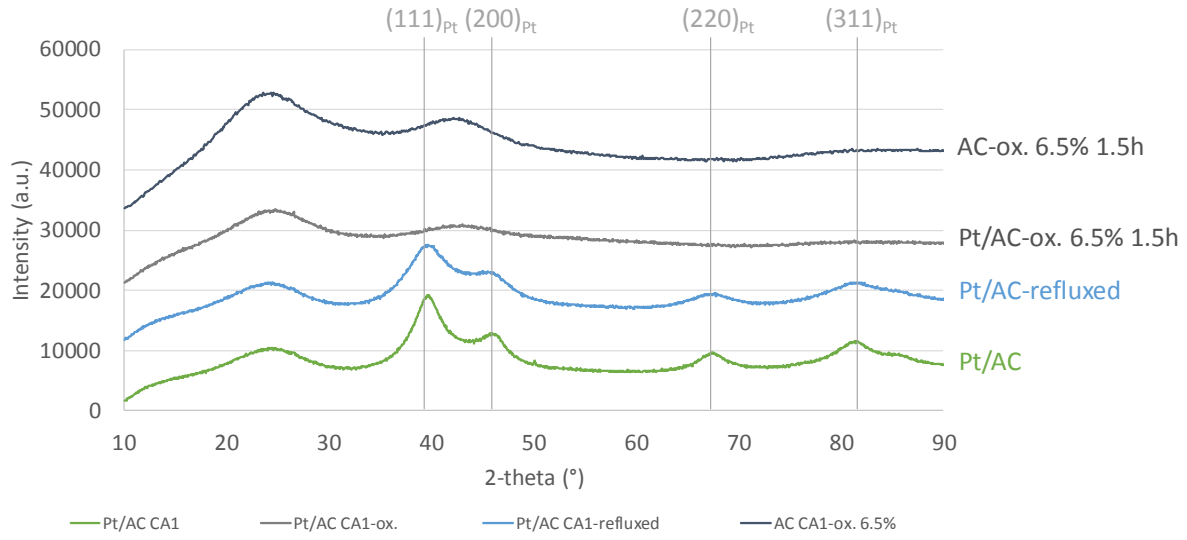

Figure 15. XRD patterns of Pt catalyst supported on different treated **CA1** supports. AC support was also characterized in order to compare XRD pattern of the catalyst with its corresponding support material.

The diameter of the platinum was roughly determined at the peak at 70 degrees 2-Thera (Table 4). Sharp peaks in the XRD diffractogram result in larger particles, while broad peaks indicate a smaller particle size. In Table 4, it can be seen that the particles of the Pt/AC CA1 are larger than those of Pt/AC CA1-refluxed. Due to the broad peaks present for the Pt/AC CA1-ox., it was not possible to produce a clear peak and calculate the average size of platinum particles.

Table 4. Particle size obtained from XRD diffractogram. (n=2)

	Particle Size (nm)
Pt/AC CA1	3.8
Pt/AC CA1-ox.	Not possible to determine
Pt/AC CA1-refluxed	2.7

The XRD results indicate that the Pt/AC CA1-ox. 6.5 % either contains low Pt amounts or too small Pt particles that are not catalytic active. The low Pt amount on the oxidized CA1 could be cause by the decrease in structural functionality after the acid treatment. Whereas the small particles are due to the formation of platinum oxide.

4.6.1 Evaluation of the catalytic performance of the Pt catalyst supported on CA1

The synthesized catalysts supported by original CA1, refluxed CA1 and oxidized CA1 were characterized by XRD and the activity was measured by titration of the formed acid.

It was shown that for the activity of the catalyst supported by the oxidized AC is lower than those prepared on original or refluxed support. Based on the XRD data, there are two possible explanations for the catalytic deactivation occurring during this oxidation:

(i) A low amount of platinum is attached to the support. This can be explained due to the significant decrease in surface area and pore volume after the HNO_3 oxidation treatment. The BET of the AC CA1-ox. was reduced by 58% and was 423 m^2/g after the acid treatment.

(ii) Due to a small size, the particles are more prone to over-oxidation on the surface and that leads to the inactivation of the catalyst. This means that either the platinum surface is covered with strongly absorbed oxygen or that surface platinum oxide is formed.[65, 66]

Analysing those to possibilities, it can be assumed that the second explanation might be more reasonable. Although the BET surface area do significant decrease, 423 m^2/g should provide enough surface area for the attachment of platinum during impregnation. Therefore, it is assumed that the catalyst deactivation occurring in this glucose oxidation can be explained due to the formation of platinum oxide.

5 Results & Discussion 2

5.1 The role of surface oxygen group on glucose oxidation over platinum catalyst

In this section, the results for the catalyst supported on SX Ultra with different amount of oxygen groups are shown. Firstly the support characterization using N_2 physisorption and TPD are presented and secondly the catalyst characterization data obtained by TEM, XRD and chemisorption are shown and discussed. The catalytic activity and selectivity were investigated for glucose oxidation in a batch reactor. Based on all these data, the support effects on the selective oxidation are analyzed and evaluated.

5.2 Support characterization

It has been reported in many works that ACs support can be modified by HNO_3 treatments to introduce oxygen groups on the carbon surface with no major changes in their textural properties.[59, 67, 68] In chapter 4 it was shown that the textural properties of the SX Ultra treated with 6.5 % (v/v) HNO_3 for 1.5 h did not change after the acid treatment. However, the oxygen density did not increase significantly in comparison to the original carbon. In was further shown, that with increasing HNO_3 concentration the density of the oxygen increases, while the textural properties decreases. Since one of the aims of this project is to chemically modify the AC by increasing the oxygen density on the support surface without altering the structure of the carbon, first the acid treatment was firstly optimized for the SX Ultra carbon. Two parameters were varied for the investigation of the acid treatment: the HNO_3 concentration and the treatment time. In an attempt to increase the amount of oxygen group without substantial support degradation the oxidation treatments were performed with two concentration for various times. It is considered that the increase in treatment time also leads to an increase in oxygen density. Table 5 summarizes the surface modification treatments carried out on AC SX Ultra. All the samples were characterized and compared during this section.

Table 5. Summary of the treatments conditions of the SX Ultra supports.

	Sample Name	HNO3 Concentration	Refluxing time
SX Ultra	AC-ox. 6.5 % 1.5 h	6.5 %	1.5 h
	AC-ox. 6.5 % 3 h	6.5 %	3.0 h
	AC-ox. 6.5 % 6 h	6.5 %	6.0 h
	AC-ox. 12 % 0.5 h	12.0 %	0.5 h
	AC-ox. 12 % 1.5 h	12.0 %	1.5 h
	AC-ox. 12 % 3 h	12.0 %	3.0 h

5.2.1 Physical characterization of the activated carbon support SX Ultra

To obtain information about the effect of HNO_3 treatment on the structure of the AC, N_2 physisorption was performed. The isothermal adsorption measurements can provide a fairly complete picture of the pore size distribution of the supports. The adsorption/desorption isotherms of the carbons are of types I and IV as defined by the IUPAC classification (Figure 16). Type I is characteristic for a microporous absorbent, while type IV represents adsorption profiles with hysteresis. The hysteresis loop between

the adsorption and desorption is relatively small and becomes narrower with higher relative pressure which indicates the presence of mesoporous structures for all carbons.

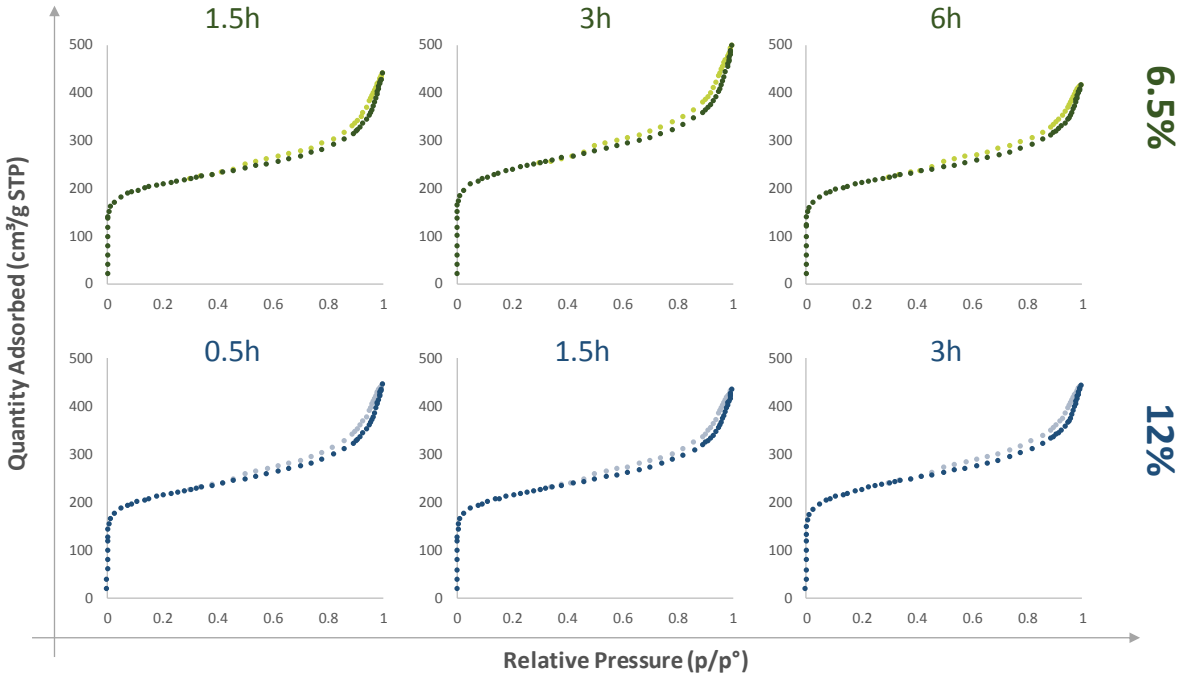

Figure 16. Adsorption/desorption isotherm profiles of SX Ultra taken by N_2 physisorption at different times.

The structural parameters calculated from the isotherms, such as BET surface area, total volume and the micro- and mesopore volumes, are shown in Table 6. In general, it can be said that the micropore volumes derived from the t-plot are smaller than the mesoopore volumes, which is typical for AC.[69] The original SX Ultra has a BET surface area and total pore volume of 789 m^2/g and 0.51 cm^3/g, respectively. The apparent BET surface area range of 700 to 1000 m^2/g with standard variation in this range. Also from this result can be deduced that the HNO_3 treatment does not drastically change the textural properties of the AC.

In other words, after the acid treatments, the physical properties do not change noticeably in comparison with the original carbon, indicating that no collapse of the pores occurs and the carbon remains stable.

Table 6. Textural properties of different SX Ultra activated carbons; all measurements were conducted three times and the average is shown (n=3).

Sample name	BET surface area (m^2/g)	Total pore volume (cm^3/g)	Micropore volume (cm^3/g)	Mesopore volume (cm^3/g)
AC-ox. 6.5 % 1.5 h	715 ± 82	0.46 ± 0.06	0.19	0.35
AC-ox. 6.5 % 3 h	949 ± 161	0.61 ± 0.10	0.26	0.40
AC-ox. 6.5 % 6 h	759 ± 19	0.48 ± 0.01	0.20	0.33
AC-ox. 12 % 0.5 h	807 ± 72	0.52 ± 0.04	0.22	0.37
AC-ox. 12 % 1.5 h	787 ± 10	0.50 ± 0.01	0.22	0.32
AC-ox. 12 % 3 h	849 ± 46	0.54 ± 0.03	0.23	0.36

5.2.2 Surface chemical characterization of the activated carbon support SX Ultra by TPD

The characterization of surface oxygen groups was done with TPD-MS by monitoring the CO and CO_2 release upon heating the carbon supports. In Figure 17 and Figure 18, the MS spectra obtained from the 6.5 % (v/v) and 12 % (v/v) HNO_3 treated carbons are shown. The grey line representing the SX Ultra-refluxed indicates a low CO and CO_2 release. In contrast, the HNO_3 treated carbons marked in green and blue have an increased CO and CO_2 release. The results show that both with increasing treatment duration and HNO_3 concentration the CO and CO_2 release rises. Since the CO and CO_2 release is an indicator for the quantity of decomposed oxygen groups on the surface, it can be stated that a higher the ion current of CO and CO_2, correspond to more oxygen groups presented on the carbon support.

In chapter 3, a trend of the CO and CO_2 evolving according to Figueiredo et al. has been explained. It shown that the CO_2 releases at lower temperatures ranges, while the CO releases at higher temperatures, which is confirmed by the obtained MS spectra.[60] The CO_2 decomposition exhibits three peaks, the first one referring to the carboxylic acids at 100–450 °C, the second one to the anhydrides at 350–600 °C, and the third one to the lactone 550–800 °C. Similarly, the CO profile shows three peaks corresponding to anhydrides, phenols and carbonyl-quinones.[47, 60-62]

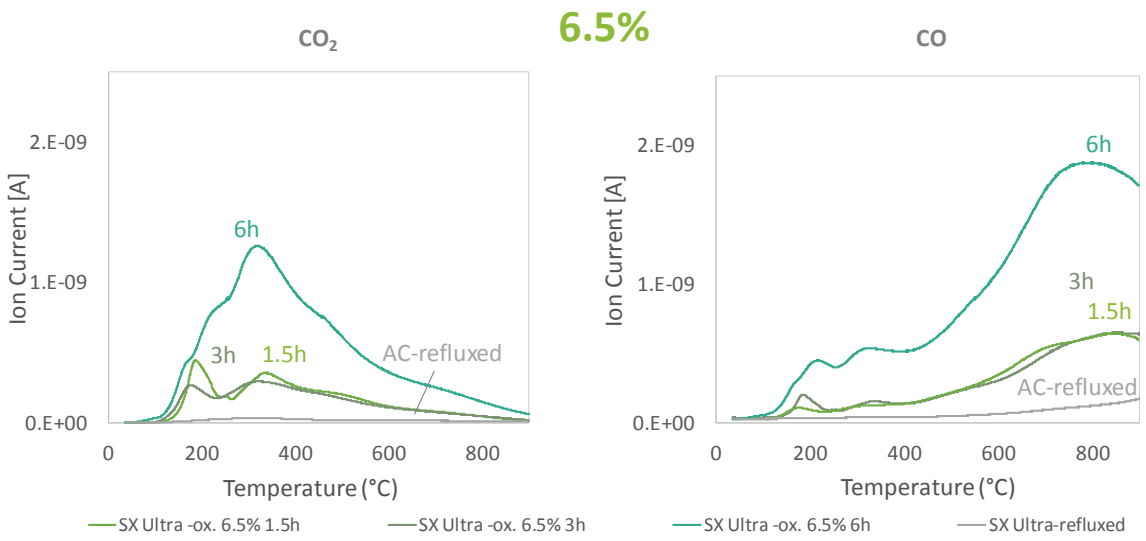

Figure 17. MS CO_2 (left) and CO (left) spectra of the SX Ultra before and after oxidation treatment; spectra shown for supports treated with 6.5 % (v/v) HNO_3 for different treatment times.

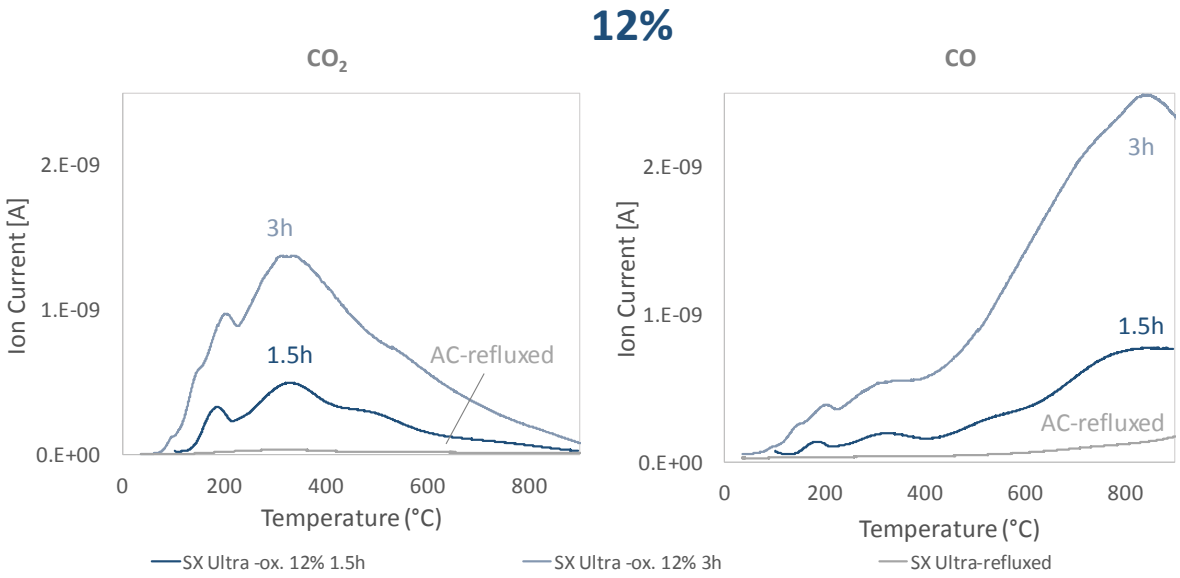

Figure 18. MS CO_2 (left) and CO (left) spectra of the SX Ultra before and after oxidation treatment; results shown for supports treated with 12 % (v/v) HNO_3 for different treatment times.

In addition to the characterization of the oxygen-containing groups, this TPD-MS was carried out to estimate the amount of introduced oxygen groups. This can be determined by the integration of the component peak areas. Table 7 shows the results obtained.

These result all clearly show that with increasing acid concentration and treatment duration the CO and CO_2 concentration increases. The CO_2 and CO concentration were the lowest for the SX Ultra-reflux and the highest for the SX Ultra-ox. 12 % 3 h. This CO and CO_2 concentration range is in line with the literature.[47, 59, 70] According to Aksoylu, the CO and CO_2 concentration of the AC Norit ROX is 0.61 mmol/g and 0.11 mmol/g, respectively. In addition, it was also demonstrated that HNO_3 oxidation led to drastic increases in both CO and CO_2 releasing groups. For the AC Norit ROX oxidized with 5 M HNO_3 for 3 hours a CO concentration of 3.62 mmol/g and a CO_2 concentration of 1.8 mmol/g was observed.[47]Calibration curves of the CO and CO2 can be find in the Appendix VII.

Table 7. Surface oxygenated groups of the AC samples.

	CO_2 (mmol/g)	CO (mmol/g)
SX Ultra-ox. 6.5 % 1.5 h	0.66	0.10
SX Ultra-ox. 6.5 % 3 h	0.55	0.09
SX Ultra-ox. 6.5 % 6 h	2.19	0.34
SX Ultra-ox. 12 % 1.5 h	0.85	0.12
SX Ultra-ox. 12 % 3 h	2.86	0.42
SX Ultra-refluxed	0.06	0.01

The TPD-MS results of SX Ultra-ox. 12 % 0.5h are not shown because the MS measurements of this sample gave a rather doubtful result due to a unknown experimental error and were therefore not taken into account. From the TPD profiles shown in Appendix VIX however, it can be seen that the data are in line with the general trend: HNO_3 oxidation led to an increase of surface oxygen groups.

5.2.3 Evaluation of support characterization

An overall look at the deconvolution results clearly shows that the oxidation treatments lead to an increase in all types of oxygen groups. The parameters time and concentration of HNO_3 lead to a variety of oxygen densities on the surface. A clear trend towards a higher density can be seen when increasing the HNO_3 concentration and the treatment time. In addition, the physisorption results show that the physical properties of the carbons were not affected by the HNO_3 treatment.

As mentioned before, one goal of this project was to increase the oxygen density on the support surface without altering the structure of the carbon. All modified supports comply with this condition and therefore could be used as support material. However, for the catalyst preparation only the SX Ultra-ox. 6.5 % 3 h and the SX Ultra-reflux were chosen as support materials. Catalysts synthesised with the SX Ultra-12 % 1.5 h were also tested on their glucose oxidation performance. The results of which can be found in Appendix IX.

5.3 Catalyst characterization

The Pt/AC catalysts with 5 wt.% platinum loading were synthesized by an impregnation method with Pt precursor $[Pt(NH_3)_4](NO_3)_2$ (Appendix X). Previous studies have shown that a calcination treatment before the reduction influences the Pt/AC structure[71] and the oxidation performance.[22] During calcination the impregnated catalyst is heated up in air, which leads to the thermal decomposition of the precursor. The decomposition temperature of the amine precursor was determined to be 250 °C (Appendix I). In the present work, the influence of calcination on the catalytic properties, such as Pt size and dispersion, and the catalytic behavior of the activated carbon-supported Pt catalysts has been studied as well. To this end, four catalysts were prepared, see Table 8.

Table 8. 5 wt.% Pt supported on different ACs; catalyst (a) was prepared from refluxed SX Ultra and is non-calcined, while (b) is calcined; catalyst (c) was prepared on SX Ultra carbon oxidized with 6.5 % HNO_3 for 3 hours, while (d) was calcined.

	Sample Name	Used support
(a)	Pt/AC	SX Ultra-refluxed
(b)	Calcined Pt/AC	SX Ultra-refluxed
(c)	Pt/AC-ox.	SX Ultra-ox. 6.5 % 3 h
(d)	Calcined Pt/AC-ox.	SX Ultra-ox. 6.5 % 3 h

The catalyst characterization was done by TEM, chemisorption and XRD in order to determine the Pt particle diameter, particle size distribution and the dispersion. The main features of the catalyst prepared are summarized in Table 10.

5.3.1 TEM

TEM is a well-established method for catalyst characterization. With TEM measurements topographic and crystallographic information, including particle size distribution, of the catalyst can be obtained.

The TEM characterization shown in Figure 19 reveals that the Pt/AC catalysts contain Pt particles with particle diameters within a relativity narrow range of 4.0 to 4.9 nm. The smallest particles (4.0 nm) were observed for the calcined Pt/AC-ox. catalyst, followed by the calcined Pt/AC with a mean diameter of 4.6 nm. Both Pt/AC and Pt/AC-ox. have an average diameter of 4.9 nm. Furthermore, the average number show no significant difference between the four catalyst. The standard deviations, minima and maxima are close in terms of values. The particle size distribution lies in a narrow range and therefore, it can be stated that the catalyst shows a homogeneous composition with no metal segregation. In the TEM images small, dark spots are visible which are the Pt nanoparticles. Due to a higher Pt electron density, the Pt particles cause a contrast compared with the AC. More TEM images are shown in Appendix XI.

From the TEM results, no significant differences in particle size can be observed. The Pt/AC catalyst has the same particle size as the Pt/AC-ox. catalyst and therefore it can be stated that the introduced oxygen groups neither have an effect on the particle size nor on the particle size distribution. In contrast, the calcined catalyst shows a smaller particle size in comparison to the non-calcined one. It was assumed that during the catalyst pretreatment in static air at 250 °C the average particle size becomes smaller, as is known from literature.[10] However, the data show no significant difference. It should also be considered that the electron microscopy does have some limitation regarding the minimum visible particle size which lies around 1 nm for our samples.[72] This limitation is also dependent on the sample preparation.

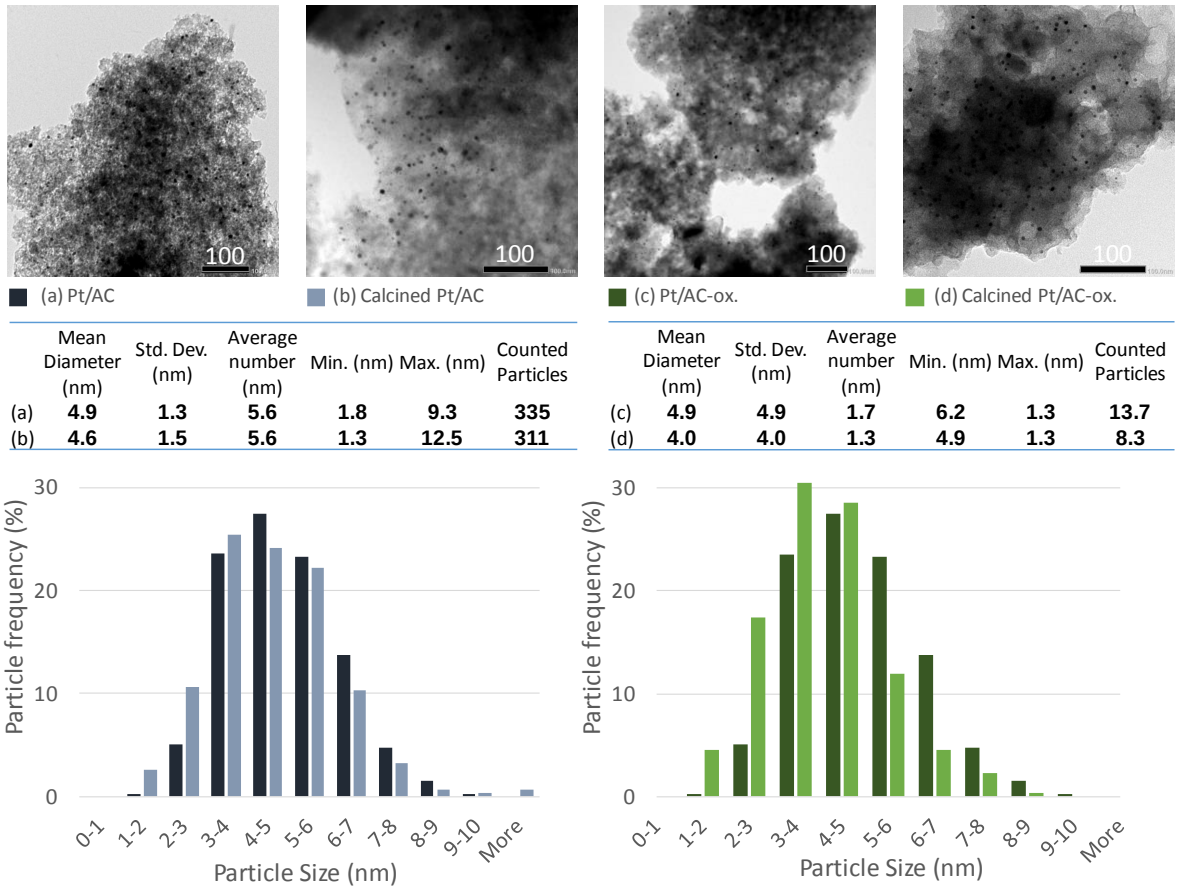

	Mean Diameter (nm)	Std. Dev. (nm)	Average number (nm)	Min. (nm)	Max. (nm)	Counted Particles
(a)	**4.9**	**1.3**	**5.6**	**1.8**	**9.3**	**335**
(b)	**4.6**	**1.5**	**5.6**	**1.3**	**12.5**	**311**

	Mean Diameter (nm)	Std. Dev. (nm)	Average number (nm)	Min. (nm)	Max. (nm)	Counted Particles
(c)	**4.9**	**4.9**	**1.7**	**6.2**	**1.3**	**13.7**
(d)	**4.0**	**4.0**	**1.3**	**4.9**	**1.3**	**8.3**

Figure 19. Representative TEM images and Pt/AC particle size distribution obtained for (a) non-calcined Pt catalyst supported on SX Ultra-reflux, (b) calcined Pt catalyst supported on SX Ultra-reflux, (c) non-calcined Pt catalyst supported on SX Ultra-ox. 6.5 % 3h and (d) calcined Pt catalyst supported on SX Ultra-ox. 6.5 % 3h.

5.3.2 Chemisorption

To obtain more information about the Pt particles of the series of Pt/AC catalysts, chemisorption was employed. The chemisorption results shown in Table 9 were taken by static chemisorption. Also pulse chemisorption with CO and H_2 was carried out to investigate the commercial catalyst (5 wt.% Pt on AC) and the synthesized 5 wt.% Pt catalyst supported on SX Ultra-refluxed. However, these measurements are difficult to interpret due to the presence of oxygen as shown in Appendix XII. Before measuring the sample, the program of static chemisorption was first validated by measuring a reference sample and the commercial catalyst (5 wt.% Pt on AC). This results can be found in Appendix XIII.

The results of the chemisorption data in Table 9 show smaller particle size for the calcined catalyst and larger parties for a non-calcined catalyst. Consequently, the dispersion is higher for the calcined catalyst and lower for the non-calcined catalyst. The largest particle size was observed for the Pt/AC-ox. and the smallest for the calcined Pt/AC-ox. This indicates that the oxygen surface groups have no effect on the particle size, which agrees with the TEM data, whereas the calcining step leads to an increase in particle size.

Table 9. Chemisorption data, including metal dispersion, particle size and quantity adsorbed, of the Pt/AC catalyst supported on different supports, obtained by static chemisorption.

	Samples	Metal Dispersion (%)	Crystallite Size (nm)	Quantity Adsorbed (µmol/g)	n*
(a)	Pt/AC	48.1 ± 1.8	2.4 ± 0.12	61.7 ± 2.3	3
(b)	Calcined Pt/AC	61.7 ± 2.0	1.8 ± 0.06	79.0 ± 2.5	2
(c)	Pt/AC-ox.	37.8 ± 3.2	3.0 ± 0.25	48.4 ± 4.0	2
(d)	Calcined Pt/AC-ox.	69.7 ± 2.2	1.6 ± 0.05	89.3 ± 2.8	2

* n = number of measured samples that passed the leak test (max. 13 µm Hg/min)

5.3.3 XRD

The catalyst was analyzed with XRD from 10° to 80° 2-Theta. As mentioned before, the SX Ultra is contaminated with silica, the XRD peaks of which unfortunately overlap with those of platinum. This makes it difficult to determine the platinum peaks and the particle size. However, regarding the major platinum peaks at 39.8° 2-Theta, a trend can be deduced from the peak width. It can be seen that Pt/AC-ox. and Pt/AC have broader peaks than the calcined catalysts.

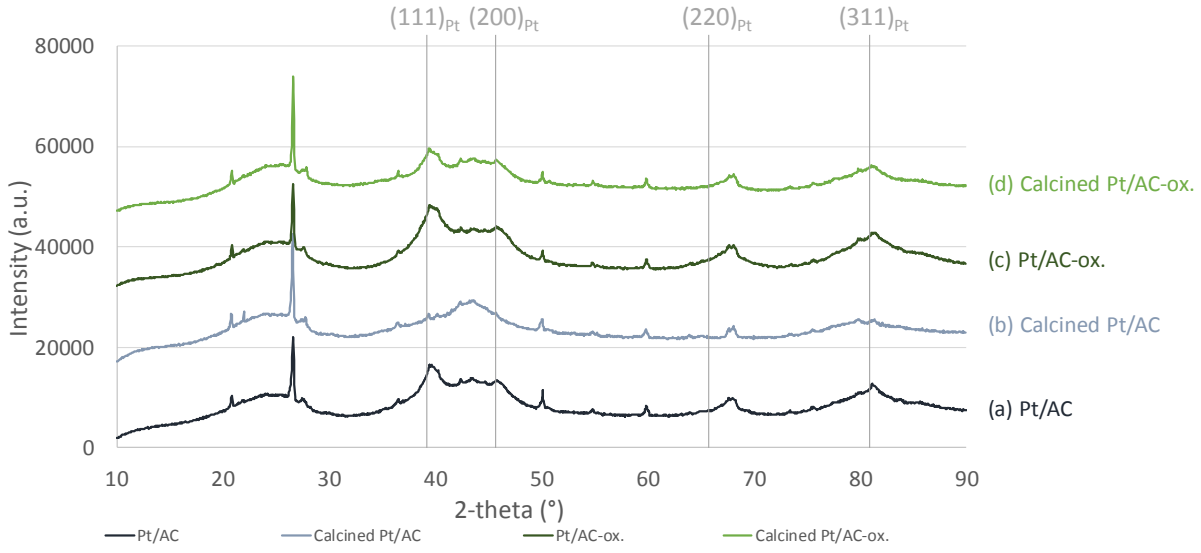

Figure 20. XRD patterns of the Pt catalyst supported on differently treated SX Ultra supports.

The platium crystallite sizes (LVol-IB) were calculated by fitting the experimental data in TOPAS and are shown in Table 10. The particle size decreases in order of Pt/AC-ox. > Pt/AC > calcined Pt/AC-ox. > calcined Pt/AC. Again the calcined catalyst indicated to have the smallest particle size. The values are within such a small range that these data are rather doubtful. However, the trend this values show, is reliable since the same can be overserved for the XRD patterns.

5.3.4 Conclusion of the catalyst characterization

The particle size obtained from the three different characterization techniques is summarized in Table 10. Both chemisorption and XRD (and to a lesser extend TEM) show that if the catalyst was pretreated

in static air at 250 °C, the particle size becomes smaller. The calcination leads precursor decomposition which seems to lead to the formation of Pt nanoparticles with smaller size. It is assumed that the interaction between the Pt particles and the support increases after precursor decomposition.

As mentioned during the introduction, it was expected that the oxidation treatment enhances the Pt dispersion so that the particle size becomes smaller. This assumption was made because the oxygen groups on the support surface form anchoring sites for the Pt metal. However, based on the shown data no clear effect of the oxygen groups on the particle size and particle size distribution can be observed.

Table 10. Main characteristics of the Pt/AC catalyst supported on different supports.

	Samples	TEM	XRD	Chemisorption
		Particle size (nm)	Particle size (nm)	Particle size (nm)
(a)	Pt/AC	4.9	1.5	2.5
(b)	Calcined Pt/AC	4.6	0.9	1.9
(c)	Pt/AC-ox.	4.9	2.2	3.2
(d)	Calcined Pt/AC-ox.	4.0	1.3	1.7

5.4 Glucose oxidation with an SX Ultra supported platinum catalyst

To evaluate the catalytic performance, the glucose oxidation was conducted using the four different catalysts in the liquid phase oxidation under standard conditions of the heterogeneous oxidation set up 2 (Chapter 2.x) . Before executing the experiments with the synthesized catalyst, the reaction set up was optimized in order to minimize gas-liquid diffusion limitation. Based on the obtained results presented in Appendix II, it can be assumed that the used oxidation set up is not limited by diffusion at the used stirring speed.

5.4.1 Oxidation measured by titration

The catalytic performance was measured by titration of the formed acid. It is assumed that per mole of acid formed, one mole of base (NaOH) is added to the reaction mixture. Hence, the volumetric production of gluconic acid can be calculated and gives an estimate of the catalytic performance. The oxidation results of the four different catalysts are shown in Figure 21. The highest activity can be observed for the calcined Pt/AC-ox., while Pt/AC and Pt/AC-ox. were determined to have similarly low activities. The calcined Pt/AC seem to have a similar initial oxidation rate as Pt/AC and Pt/AC-ox. However, this rate increases after 10 min and shows a small but clear difference towards the non-calcined catalyst.

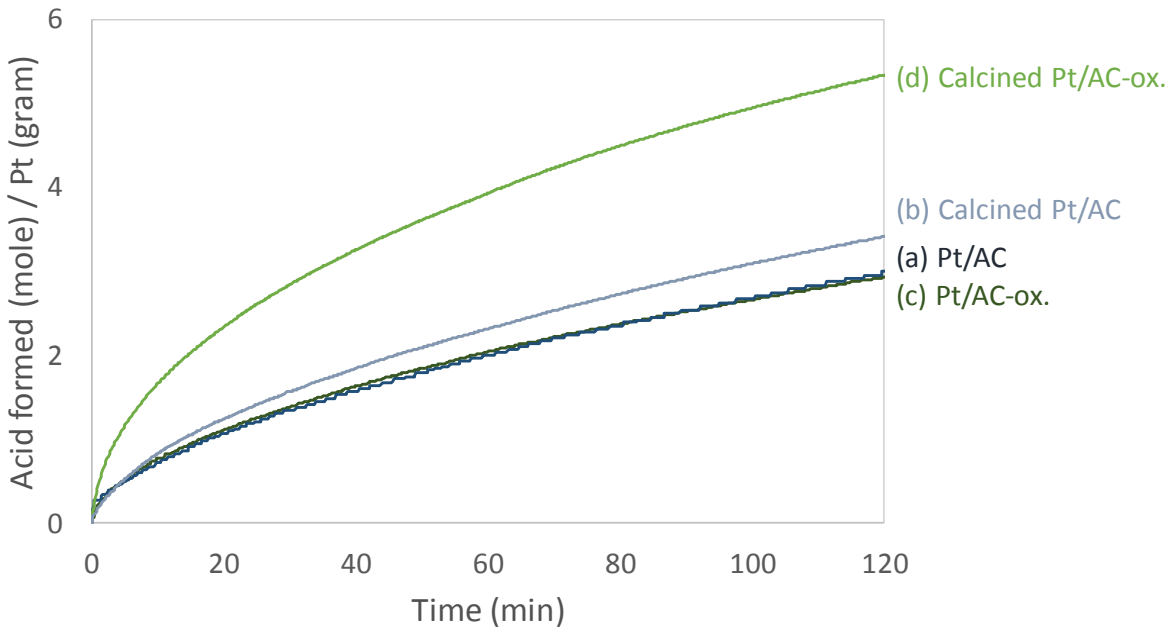

Figure 21. Glucose oxidation as measured by titration of formed acid. Reactions were performed at 50 °C, pH 9, 0.05 M substrate concentration, stirring speed of 2000 rpm and an oxygen flowrate of 300 mL/min.

In summary, calcination of the Pt catalyst support on oxidized carbon significantly enhanced the catalytic performance. An oxidation treatment of the support does not affect the catalytic activity since the activity of the Pt/AC-ox. is rather low. Furthermore, it can be concluded that the increased activity of the calcined Pt/AC-ox. does not result from the calcining pretreatment, as indicated by the low activity of the second calcined catalyst with less hydrophilic support.

5.4.2 HPLC analysis and TOF calculations

The quantification of the reaction products was performed by High-Performance Liquid Chromatography (HPLC). Table 11 gives the conversion, yield, and selectivity after 20 min of glucose oxidation. Under same reaction conditions, the calcined Pt/AC-ox. catalyst is the most effective in glucose conversion and gluconic acid production. The remaining catalysts have similar conversion rates and yield. These results are in line with those shown for the titration. A high selectivity to gluconic acid (>80 %) of all four catalysts is confirmed by the HPLC analysis. This result is in agreement with previous studies conducted on glucose oxidation with a Pt catalyst supported on AC.[22] According to Delidovich et al., the selectivity of a Pt/AC catalyst attained 95 % at a conversion efficiency of 90 % under controlled O_2-diffusion.[19, 29] A detailed study by Dirkx and Vanderbaan revealed that gluconic acid production reached a selectivity of 60-70 % and 80-90 % at low and high substrate conversions, respectively.[23] No other product aside from gluconic acid can be detected from the HPLC chorograms (Appendix XIV).

The turnover frequency was calculated according to the equation in chapter 2 and the results are shown in Table 11. The analysis shows that the calcined Pt/AC-ox. catalyst provides a substantially higher TOF compared to the other three at 10 % conversion. A similar trend can be observed for the

TOF_i of the catalysts; the catalyst a-c have a TOF_i of 0.03 s^{-1}, while the TOF_i from the d is 0.05 s^{-1}. This observation is corroborated by the results obtained by titration.

Delidovich et al. conducted glucose oxidation with Pt/AC and calculated a TOF of 0.05 s^{-1} excluding the dispersion. In comparison, the TOF calculated for Pt/AC, calcined Pt/AC, Pt/AC-ox. and calcined Pt/AC-ox. are 0.02, 0.04, 0.02 and 0.14 s^{-1}, respectively. Comotti et al. calculated a mean TOF of 60 h^{-1} (0.02 s^{-1}) for glucose oxidation over a Pt catalyst supported on carbon after a reaction time of 6.5 h.[73] These small variances in the data demonstrated by different authors can be explained by the nature of the Pt/AC catalyst used as well as different catalyst preparation procedures and reaction conditions.

Table 11. Oxidation degree of glucose oxidized with O_2 as oxidant and Pt/AC with different supports of the catalyst. Reactions were performed at 50 °C, pH 9, 0.05 M substrate concentration, stirring speed of 2000 rpm and an oxygen flowrate of 300 mL/min.

	Sample name	Conversion[a] (%)	Yield[a] (%)	Selectivity[a] (%)	TOF[b] (s^{-1})	TOF_i[c] (s^{-1})
(a)	Pt/AC	9	10	100	0.04	0.03
(b)	Calcined PT/AC	11	10	82	0.06	0.03
(c)	Pt/AC-ox.	5	8	100	0.05	0.03
(d)	Calcined PT/AC-ox.	22	21	98	0.21	0.05

[a] obtained after 20 min

[b] TOF at 10 % yield: $[TOF] = [mol_{Gluconic\ acid} * s^{-1} * mol_{Pt}^{-1} * D_{Pt}]$

[c] TOF_i after 10 min: $[TOF_i] = [R * V * mol_{Pt}^{-1} * D_{Pt}]$

5.4.3 Evaluation of the catalytic performance

The oxidation of glucose into gluconic acid over a Pt catalyst supported on carbon material can be achieved with high selectivity. The calcined Pt/AC-ox. catalyst demonstrated a substantially higher TOF in comparison to the other catalysts. Hence, a hydrophilic support in combination with a calcination step during catalyst synthesis has a positive effect on the selective glucose oxidation over Pt/Ac catalysts, which could be explained by three different reasons: adsorption of the substrate, electronic effect of oxygen groups or particle size effect in this reaction.

Both the amount and type of oxygen groups on the support determine the degree of hydrophilicity. In turn, a hydrophilic character of the catalyst will affect the affinity of the catalyst towards the substrate (substrate-catalyst interaction). Thus, the supported oxygen group might enhance the adsorption of the glucose and therefore lead to an increase in reaction rate. However, the titration and HPLC data demonstrate that for the Pt/AC-ox. neither significant increase nor decrease in reaction rate can be observed. Accordingly, the positive effect on the catalytic activity shown by calcined Pt/AC-ox. cannot be explained through the substrate-catalyst interactions.

The influence of catalyst preparation and indirectly of Pt particle sizes on catalytic performance in the glucose oxidation reaction could be another possible reason for the increase in reaction rate. The particle size effect has been subject of many studies.[26, 27, 49] Often, metal particles size and support effect occur simultaneously. This was also one of the main challenges during this project; synthesizing

a catalyst with different amounts of oxygen groups and similar Pt particle size since the surface oxygen groups form anchoring sites for the Pt. The characterization data shows that the particle size varies. However, this deviation is not caused by the introduced oxygen groups, but by calcination of the catalyst since both calcined catalysts show smaller particles for all three characterization techniques. In contrast, smaller particles do not always show the highest activity as can be seen for the calcined Pt/AC catalyst. Consequently, the rate enhancing effect is not only caused by particle size.

The positive effect on the catalytic activity with the calcined PT/AC-ox. may result from an electronic effect of the support. The differences in number and nature of the oxygen groups may affect the electronic state of the platinum. The electrons are transferred from the carbon support to the edges of platinum which are the active sites of the catalyst.[26] A higher electron density in the active sites could be one of the reasons for the increase in reaction rate. There are two possibilities considered in which the electronic effect could enhance the reaction rate:

(i) Due to the small particles and the oxygen groups on the calcined Pt/AV-ox. the electronic effect is stronger. In other words, small particles are more sensitive to electronic effects of the support, and since oxygen groups enhance the electronic effect, the combination of those leads to this significant increase in reaction rate. The remaining three catalysts either have a larger particle size or do contain a lower oxygen density. Therefore, the electronic effect of the support for those catalysts is less intensive limiting the catalytic activity.

(ii) The calcination might influence the platinum-support interaction. Due to the calcination, the platinum binds differently to the support whereby more electrons can be transferred, and the reaction rate is increased.

In summary, the introduction of surface oxygen groups only resulted in a substantial increase in activity when the catalyst calcined prior to the reduction step. No effect of surface oxygen groups on the activity was observed when the calcination step was omitted. These differences cannot be explained by substrate-catalyst interaction nor by particle size only. An electronic effect from the surface oxygen groups only noticeable in the case the Pt particles are very small which was the result of the calcination treatment could be an explanation for the high catalytic activity. This has not been proven but it is a plausible explanation.

6 Conclusion and recommendations

6.1 Conclusion

In this work, the role of support oxygen groups on the catalytic performance of platinum on activated carbon (Pt/AC) in selective glucose oxidation has been established. Catalysts with two different oxygen densities (Pt/AC and Pt/AC-ox) have been synthesized and compared with regard to their catalytic activity. First, a series of AC were oxidized by refluxing in HNO_3 mixtures for different periods of time. N_2 physisorption and TPD-MS were used to characterize the chemical and physical properties of the treated and the untreated AC. Four different catalysts were prepared by using incipient wetness impregnation with $[Pt(NH_3)_4](NO_3)_2$ as a precursor. Two catalysts were directly reduced and the other two were first calcined. All catalysts were tested in a liquid phase reaction and they successfully oxidized glucose into gluconic acid. Finally, it has been found out that the supported oxygen groups only have an enhanced effect on the catalytic performance after previous calcination of the catalyst.

A comparative study of the two activated carbons SX Ultra and CA1 has been done. Both carbons were oxidized in HNO_3 for different concatenation and treatment times. The textural properties of the carbons change with the severity of the acid treatment. SX Ultra has a much more stable physical structure after the oxidation treatments compared with the CA1. In addition, TPD-MS results demonstrated an increase in the amount of oxygen-containing surface groups after the oxidative treatment. Furthermore, it has been shown that the number of oxygen-containing surface groups can be tuned by varying the treatment time and acid concertation.

According to the TEM results, each catalyst contains metallic platinum. The particle size observed with chemisorption ranged from 1.6–3.2 nm. A relationship between the particle size and the calcination treatment was observed; calcination led to an increase in particle size. Furthermore, the oxidation treatments did not enhance the dispersion of the Pt metal on AC.

The calcined Pt catalyst on an oxidized support exhibited the highest catalytic activity. The calculated TOF at 10 % conversion of glucose was 0.21 s^{-1}. The remaining three catalysts showed similar activity and had a TOF of 0.04–0.06 s^{-1}. All catalysts showed high selectivity towards gluconic acid formation.

Based on the obtained results, the significant increase in activity for the calcined catalyst on oxidized support can neither be explained with an adsorption effect nor with a particle size effect alone. It is expected that an electronic effect enhances the activity of a calcined catalyst with oxidized support. However, how this effect exactly affects the catalyst still needs to be investigated.

6.2 Recommendations

Several recommendations and improvements are suggested to continue with this research.

The introduction of surface oxygen groups was obtained by nitric acid oxidation. However, there are several other methods to introduce functional oxygen groups on a support structure, such as gas phase oxidation with oxygen, or by using other acids (H_2SO_4). Next to the oxygen groups, also nitrogen functional groups can be incorporated into the carbon materials. Surface nitrogen seems to play an important role in the catalytic activity and it might be interesting to investigate its influence on carbohydrate oxidation.

An analysis of the amount of oxygen groups on the carbon surface can be performed by MS-TPD as shown in this report, or with titration. During this study, several titrations were performed with the aim to calculate an exact amount of oxygen groups. For time reasons, the titration study could not be continued but should be further investigated.

Furthermore, the effect of carbohydrates with higher molecular weight on the catalytic performance of Pt/AC catalyst should be investigated. Carbohydrates such as maltose and maltotriose could be used as substrates for this purpose.

The electronic effect on the glucose oxidation should be analyzed. This needs to be done to understand the increase in reaction rate of the calcined Pt/AC catalyst with a high oxygen support content in comparison to the non-calcined catalyst and the one with low oxygen support content.

7 Acknowledgement

I would like to say thanks to the chair group and laboratory of Biobased Chemistry and Technology (BCT) for hosting and helping me during my master thesis.

I especially would like to thank the chairholder prof. dr. Harry Bitter for giving me the possibility to do my thesis at BCT. His supervision of my thesis and the inspiring discussions were very helpful (and were strongly appreciated.) and significantly contributed to the quality of this report.

Also, my special thanks go to Tomas van Haasterecht for his supervision and frequent consultation in the lab. His dedication, patience and advices helped me during my research and steered me towards the right direction till completion. Thanks, for the good cooperation, which made my stay and work more pleasant.

In addition, I would like to thank Evie van der Wijst for the supervision and the establishment of this thesis project. Through her I got into touch with BCT, for which I am very grateful.

Finally, I want to acknowledge Mirka, Sophie, Lara and the thesis ring as the readers of this thesis. Your corrections and advises helped me writing this thesis.

I really enjoyed my stay at BCT, as well the topic of my thesis!

References

1. P. McKendry, *Bioresource Technol*, 2002, **83**, 37-46.
2. N. L. Vanier, S. L. M. El Halal, A. R. G. Dias and E. D. R. Zavareze, *Food Chem*, 2017, **221**, 1546-1559.
3. M. A. Abbas, S. Hameed and J. Kressler, *Starch-Starke*, 2013, **65**, 264-272.
4. V. K. Khlestkin, S. E. Peltek and N. A. Kolchanov, *Carbohyd Polym*, 2018, **181**, 460-476.
5. Y. J. Wang and L. F. Wang, *Carbohyd Polym*, 2003, **52**, 207-217.
6. P. Tolvanen, P. Maki-Arvela, A. B. Sorokin, T. Salmi and D. Y. Murzin, *Chem Eng J*, 2009, **154**, 52-59.
7. Y. Sheng, Q. H. Wang, X. C. Xu, W. Y. Jiang, S. C. Gan and H. F. Zou, *Lwt-Food Sci Technol*, 2011, **44**, 139-144.
8. A. B. Sorokin, S. L. Kachkarova-Sorokina, C. Donze, C. Pinel and P. Gallezot, *Top Catal*, 2004, **27**, 67-76.
9. S. R. Collinson and W. Thielemans, *Coordin Chem Rev*, 2010, **254**, 1854-1870.
10. X. L. Chen, Y. Liu, H. Wang, M. J. Yuan, X. H. Wang and Y. G. Chen, *Rsc Adv*, 2014, **4**, 11232-11239.
11. X. D. Zhang and W. L. Li, *J Appl Polym Sci*, 2003, **88**, 1563-1566.
12. G. Guclu, E. Al, S. Emik, T. B. Iyim, S. Ozgumus and M. Ozyurek, *Polym Bull*, 2010, **65**, 333-346.
13. M. Zhou, J. Z. Zhao and L. Z. Zhou, *J Appl Polym Sci*, 2011, **121**, 2406-2412.
14. B. Achremowicz, D. Gumul, A. Bala-Piasek, P. Tomasik and K. Haberko, *Carbohyd Polym*, 2000, **42**, 45-50.
15. T. Salmi, P. Tolvanen, J. Warna, P. Maki-Arvela, D. Murzin and A. Sorokin, *Chem Eng Sci*, 2016, **146**, 19-25.
16. L. H. Garrido, E. Schnitzler, M. E. B. Zortea, T. D. Rocha and I. M. Demiate, *J Food Sci Tech Mys*, 2014, **51**, 2640-2647.
17. P. L. Bragd, A. C. Besemer and H. van Bekkum, *Carbohyd Res*, 2000, **328**, 355-363.
18. D. J. Cole-Hamilton, *Science*, 2003, **299**, 1702-1706.
19. M. Besson, P. Gallezot and C. Pinel, *Chemical Reviews*, 2014, **114**, 1827-1870.
20. P. Gallezot, *Catal Today*, 1997, **37**, 405-418.
21. Z. H. Zhang and G. W. Huber, *Chem Soc Rev*, 2018, **47**, 1351-1390.
22. M. Linders, E. v. d. Wijst and H. Bitter, 2017.
23. J. M. H. Dirkx and H. S. Vanderbaan, *J Catal*, 1981, **67**, 1-13.
24. D. L. Verraest, J. A. Peters and H. van Bekkum, *Carbohyd Res*, 1998, **306**, 197-203.
25. J. H. Vleeming, B. F. M. Kuster and G. B. Marin, *Carbohyd Res*, 1997, **303**, 175-183.
26. J. H. Vleeming, B. F. M. Kuster and G. B. Marin, *Catal Lett*, 1997, **46**, 187-194.
27. T. Haynes, V. Dubois and S. Hermans, *Journal*, 2017, **542**, 47-54.
28. M. Besson, G. Fleche, P. Fuertes, P. Gallezot and F. Lahmer, *Recl Trav Chim Pay B*, 1996, **115**, 217-&.
29. I. V. Delidovich, O. P. Taran, L. G. Matvienko, A. N. Simonov, I. L. Simakova, A. N. Bobrovskaya and V. N. Parmon, *Catal Lett*, 2010, **140**, 14-21.
30. Y. Onal, S. Schimpf and P. Claus, *J Catal*, 2004, **223**, 122-133.
31. L. S. Ribeiro, E. G. Rodrigues, J. J. Delgado, X. W. Chen, M. F. R. Pereira and J. J. M. Orfao, *Ind Eng Chem Res*, 2016, **55**, 8548-8556.
32. A. Mirescu and U. Prusse, *Appl Catal B-Environ*, 2007, **70**, 644-652.
33. S. Solmi, C. Morreale, F. Ospitali, S. Agnoli and F. Cavani, *Chemcatchem*, 2017, **9**, 2797-2806.
34. R. Yulina, E. v. d. Wijst and H. Bitter, 2016.
35. R. Garcia, M. Besson and P. Gallezot, *Appl Catal a-Gen*, 1995, **127**, 165-176.
36. T. Mallat and A. Baiker, *Catal Today*, 1994, **19**, 247-283.
37. E. Lam and J. H. T. Luong, *Acs Catal*, 2014, **4**, 3393-3410.
38. D. Morales-Acosta, F. J. Rodriguez-Varela and R. Benavides, *Int J Hydrogen Energ*, 2016, **41**, 3387-3398.
39. E. Perez-Mayoral, V. Calvino-Casilda and E. Soriano, *Catal Sci Technol*, 2016, **6**, 1265-1291.
40. E. Auer, A. Freund, J. Pietsch and T. Tacke, *Appl Catal a-Gen*, 1998, **173**, 259-271.
41. H. Marsh and F. Rodríguez-Reinoso, *Activated carbon*, Elsevier, Amsterdam ; Boston, 1st edn., 2006.
42. D. S. Cameron, Cooper, S. J., Dodgson, I. L., Harrison, B., & Jenkins, J. W. , 1990, **7**, 113-137.
43. I. Matos, M. Bernardo and I. Fonseca, *Catal Today*, 2017, **285**, 194-203.
44. R. W. Gosselink, W. Xia, M. Muhler, K. P. de Jong and J. H. Bitter, *Acs Catal*, 2013, **3**, 2397-2402.
45. M. L. Toebes, T. A. Nijhuis, J. Hajek, J. H. Bitter, A. J. van Dillen, D. Y. Murzin and K. P. de Jong, *Chem Eng Sci*, 2005, **60**, 5682-5695.
46. H. P. Boehm, *Carbon*, 1994, **32**, 759-769.
47. A. E. Aksoylu, M. Madalena, A. Freitas, M. F. R. Pereira and J. L. Figueiredo, *Catal Today*, 2001, **39**, 175-185.
48. L. Jiao and J. R. Regalbuto, *J Catal*, 2008, **260**, 329-341.
49. C. Zhang, T. Wang and Y. J. Ding, *Catal Lett*, 2017, **147**, 1197-1203.
50. S. E. Davis, M. S. Ide and R. J. Davis, *Green Chem*, 2013, **15**, 17-45.
51. C. Lastoskie, K. E. Gubbins and N. Quirke, *J Phys Chem-Us*, 1993, **97**, 4786-4796.
52. S. Gil, L. Munoz, L. Sanchez-Silva, A. Romero and J. L. Valverde, *Chem Eng J*, 2011, **172**, 418-429.
53. Z. A. ALOthman, *Materials*, 2012, **5**, 2874-2902.
54. K. S. P. Bertier, H. Stanjek, A. Ghanizadeh, C. R. Clarkson, A. Busch, N. Kampman, D. Prinz, A. Amann-Hildenbrand, B. M. Kross and V. Pipich, *The Clay Minerals Society*, 2016, **Vol. 21**, 151–161.
55. E. G. Rodrigues, M. F. R. Pereira, X. W. Chen, J. J. Delgado and J. J. M. Orfao, *J Catal*, 2011, **281**, 119-127.
56. W. F. Han, H. Z. Liu and H. Zhu, *Catal Commun*, 2007, **8**, 351-354.
57. A. Dandekar, R. T. K. Baker and M. A. Vannice, *Carbon*, 1998, **36**, 1821-1831.
58. F. Rodriguez-Reinoso and M. Molina-Sabio, *Adv Colloid Interfac*, 1998, **76**, 271-294.
59. C. Moreno-Castilla, M. V. Lopez-Ramon and F. Carrasco-Marin, *Carbon*, 2000, **38**, 1995-2001.
60. J. L. Figueiredo, M. F. R. Pereira, M. M. A. Freitas and J. J. M. Orfao, *Carbon*, 1999, **37**, 1379-1389.
61. J. L. Figueiredo, *J Mater Chem A*, 2013, **1**, 9351-9364.
62. J. L. Figueiredo and M. F. R. Pereira, *Catal Today*, 2010, **150**, 2-7.
63. D. W. Koppenaal, C. J. Barinaga, M. B. Denton, R. P. Sperline, G. M. Hieftje, G. D. Schilling, F. J. Andrade and J. H. Barnes, *Anal Chem*, 2005, **77**, 418a-427a.
64. R. Rizo, D. Sebastian, M. J. Lazaro and E. Pastor, *Appl Catal B-Environ*, 2017, **200**, 246-254.
65. A. P. Markusse, B. F. M. Kuster, D. C. Koningsberger and G. B. Marin, *Catal Lett*, 1998, **55**, 141-145.

66. P. J. M. Dijkgraaf, M. J. M. Rijk, J. Meuldijk and K. Vanderwiele, *J Catal*, 1988, **112**, 329-336.
67. J. H. Xu, J. Zhao, J. T. Xu, T. T. Zhang, X. N. Li, X. X. Di, J. Ni, J. G. Wang and J. Cen, *Ind Eng Chem Res*, 2014, **53**, 14272-14281.
68. A. Valente, C. Palma, I. M. Fonseca, A. M. Ramos and J. Vital, *Carbon*, 2003, **41**, 2793-2803.
69. I. I. Salame and T. J. Bandosz, *J Colloid Interf Sci*, 1999, **210**, 367-374.
70. J. M. Calo, D. CazorlaAmoros, A. LinaresSolano, M. C. RomanMartinez and C. S. M. DeLecea, *Carbon*, 1997, **35**, 543-554.
71. C. C. Shih and J. R. Chang, *Mater Chem Phys*, 2005, **92**, 89-97.
72. R. Richards, *Surface and nanomolecular catalysis*, CRC/Taylor & Francis, Boca Raton, FL, 2006.
73. M. Comotti, C. Della Pina and M. Rossi, *J Mol Catal a-Chem*, 2006, **251**, 89-92.

Appendix

I. Appendix: Calcination data

In Figure 22 the TGA data of the two precursors H_2PtCl_6 (left) and $[Pt(NH_3)_4](NO_3)_2$ (right) can be seen. H_2PtCl_6 no clear decomposition temperature can be determined, while the $[Pt(NH_3)_4](NO_3)_2$ shows one peak at 250 °C. Therefore, the calcination of the catalysts impregnated with $[Pt(NH_3)_4](NO_3)_2$ was done at 250 °C. Also for the H_2PtCl_6 was chosen to be 250 °C, since large amounts of the precursors was at this temperature decomposed.

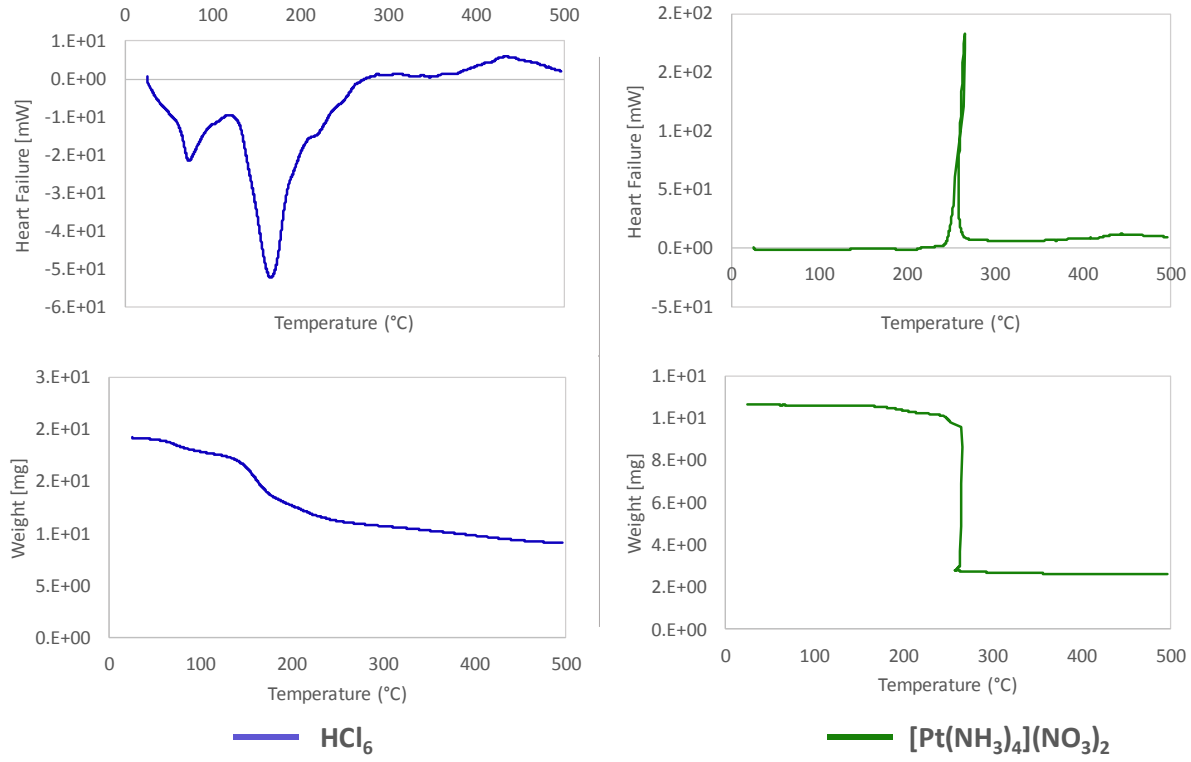

Figure 22. TGA data of the two precursors H_2PtCl_6 (left) and $[Pt(NH_3)_4](NO_3)_2$ (right). Measurements were conducted in air.

II. Appendix: Reactor optimisation

From Fig. it can be seen that there is no difference in initial reaction rate between the 1200 rpm and the 2000 rpm

Glucose oxidation as measured by titration of formed acid. 5% Pt/AC catalyst supported on SX Ultra-reflux prepared with the precursor H2PtCl6 and [Pt(NH3)4](NO3)2 .Reactions were performed at 50 °C, pH 9, 0.05 M substrate concentration, stirring speed of 2000 rpm and an oxygen flowrate of 300 mL/min.

Figure 39. Glucose oxidation as measured by titration of formed acid. The commercial catalyst 5% Pt/AC catalyst were used. Reactions were performed at 50 °C, pH 9, 0.05 M substrate concentration, stirring speed of 2000 rpm and an oxygen flowrate of 300 mL/min.

III. Appendix: TGA measurements of the four catalyst supported on CA1

The TGA data shown in Figure 23 indicates that the oxidized support has the higher weight lost. That attributed to the introduced oxygen groups. The CA1-reflux and the original CA1 do have the same weight lost.

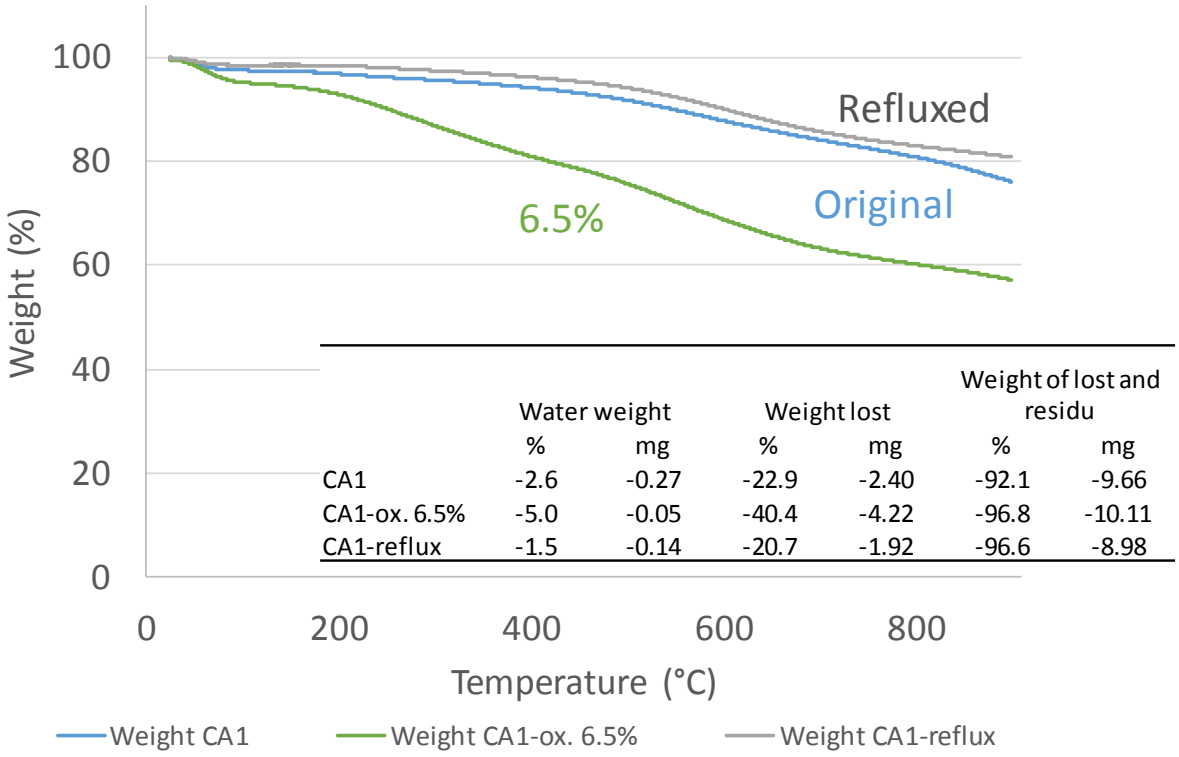

	Water weight		Weight lost		Weight of lost and residu	
	%	mg	%	mg	%	mg
CA1	-2.6	-0.27	-22.9	-2.40	-92.1	-9.66
CA1-ox. 6.5%	-5.0	-0.05	-40.4	-4.22	-96.8	-10.11
CA1-reflux	-1.5	-0.14	-20.7	-1.92	-96.6	-8.98

Figure 23. TGA data of the supports CA1, CA1-ox. 6.5% and CA1-reflux. In the table the weight lost over the heating procedure is given.

IV. Appendix: XPS wide and narrow scans

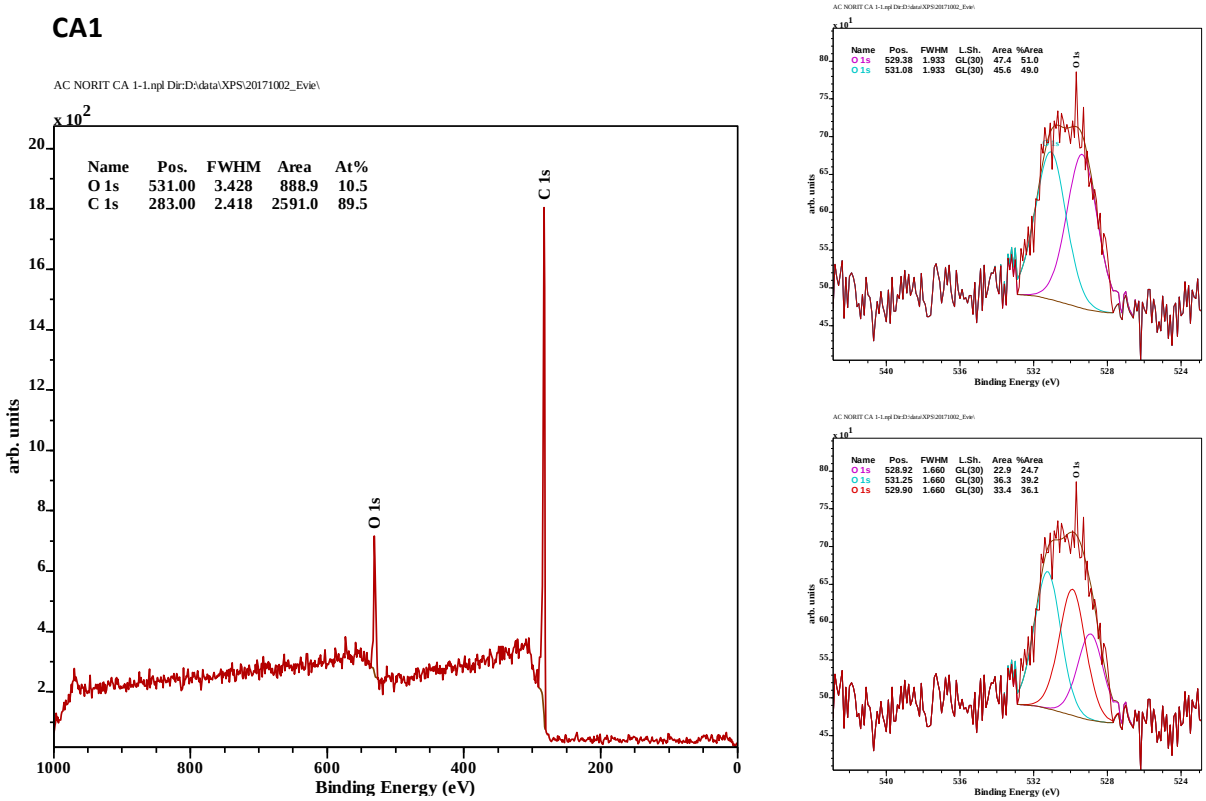

Figure 24. XPS wide (left) and oxygen narrow (right) scan of AC CA1. Two peaks can be fitted into the oxygen narrow scan. From Figueiedo (2010) found out that at 531.1 eV C=O and 532.3 eV hydroxyls, ethers and C=O in esters, amides and anhydrides are. The two oxygen groups fitted in the upper oxygen narrow scan could be attributed to those.

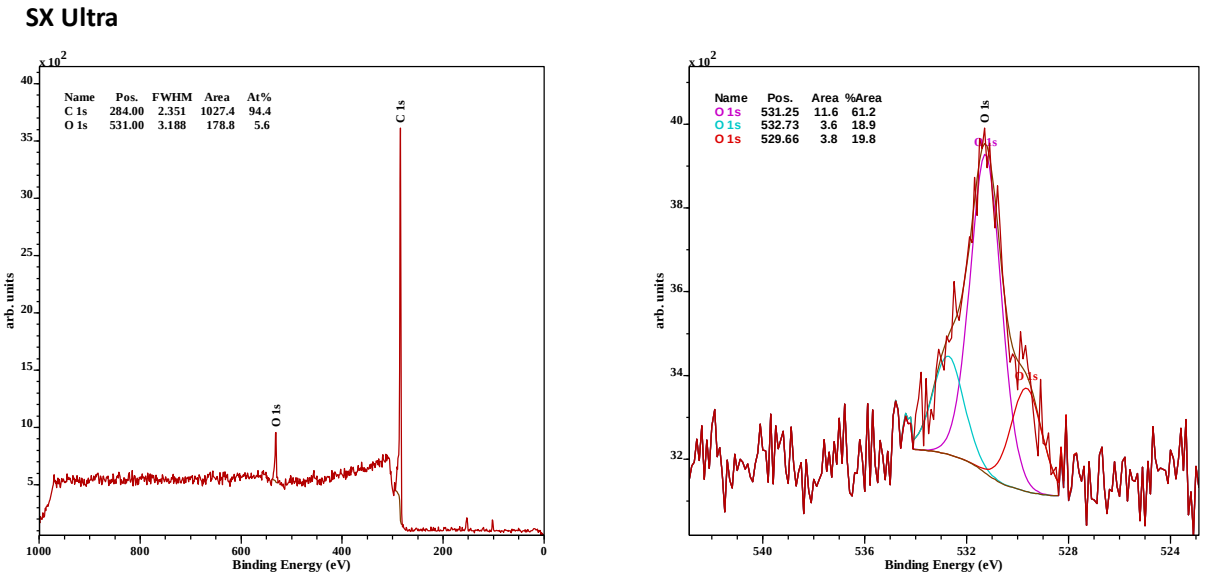

Figure 25. XPS wide (left) and oxygen narrow (right) scan of AC SX Ultra.

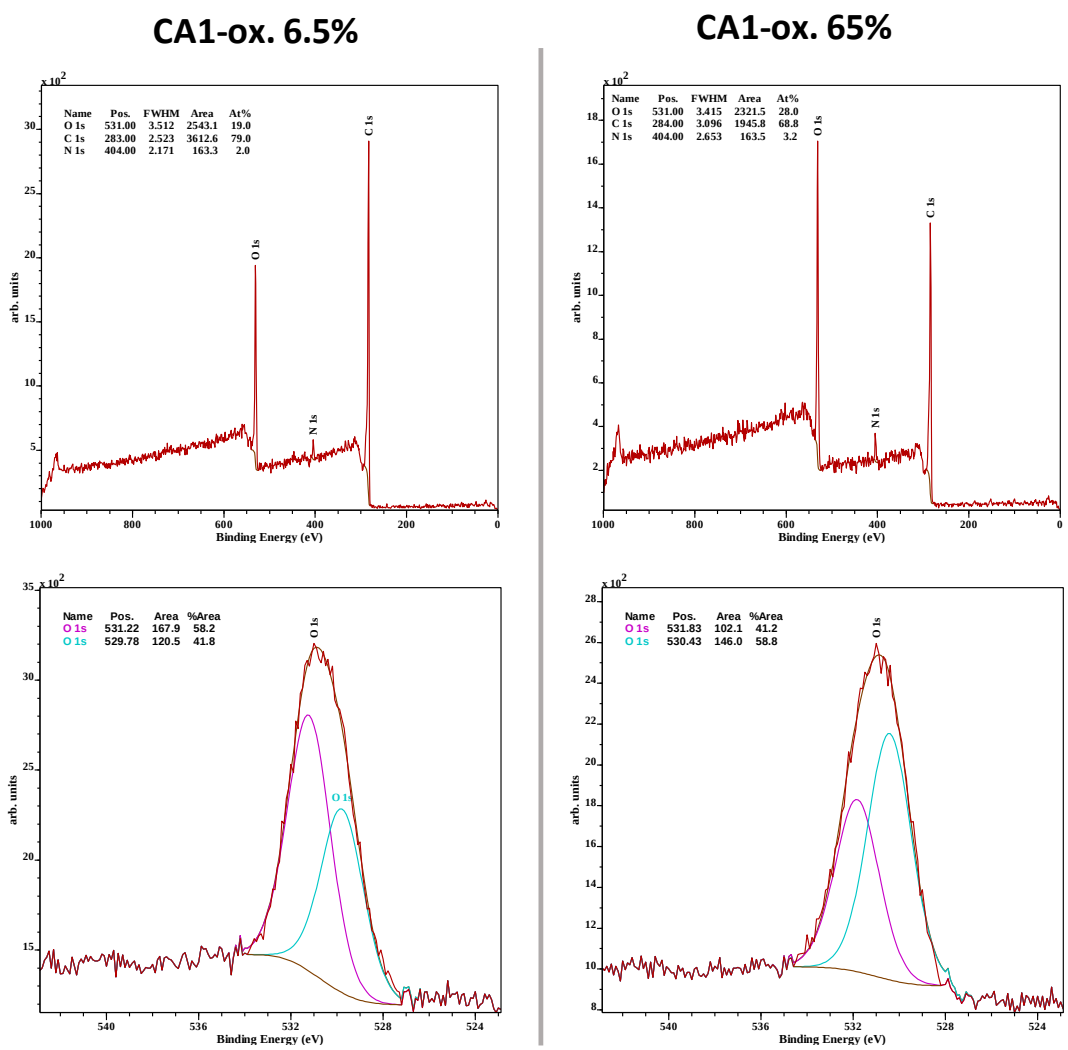

Figure 26. XPS wide (up) and oxygen narrow (down) scan of AC CA1-ox. 6.5% (left) and 65% (right).

V. Appendix: MS spectra of water at CA1

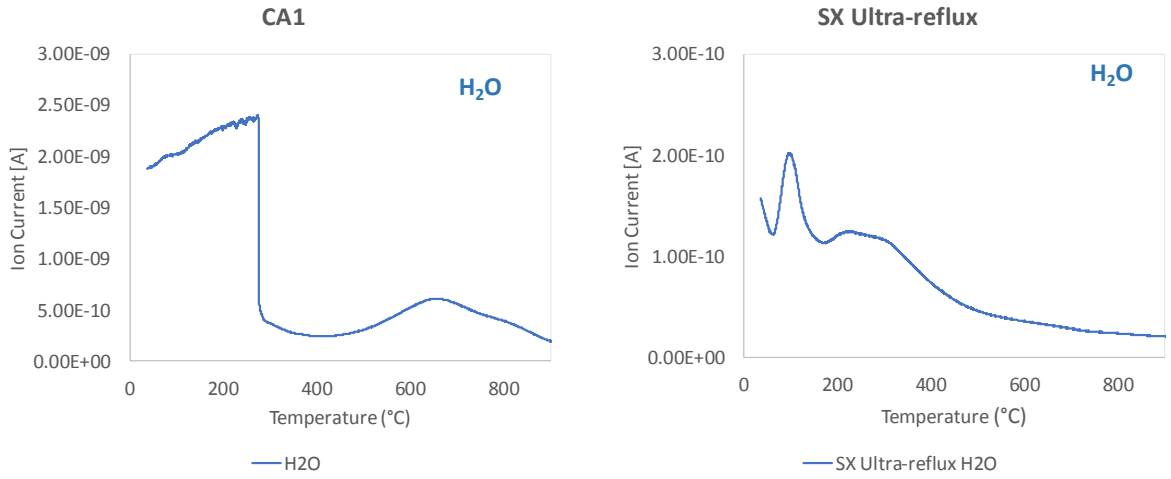

Figure 27. H_2O TPD-MS spectra in He with 10 °C/min of CA1 and SX Ultra-reflux.

VI. Appendix: MS spectra of measurements with no sample of with glass wool

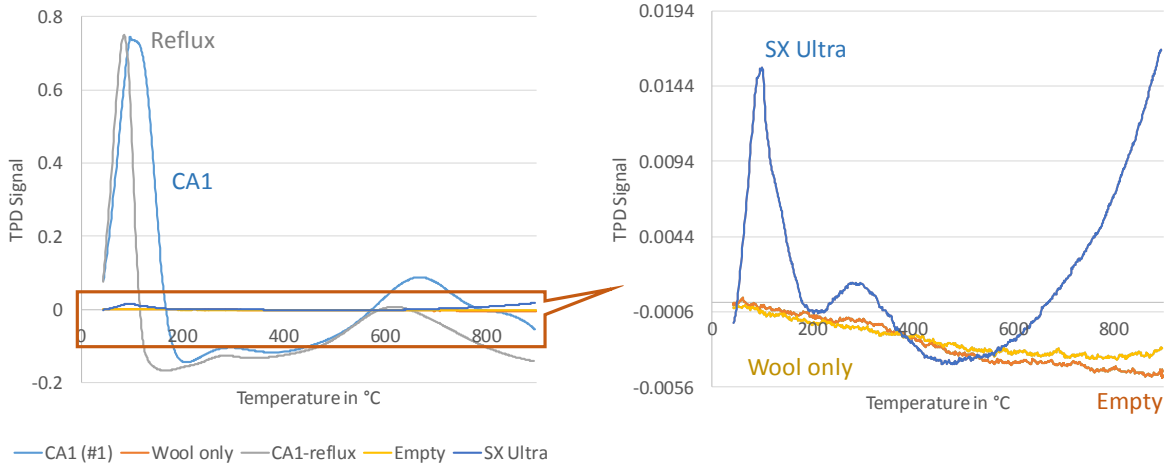

Figure 28. TPD spectra in He with 10 °C/min of CA1, Wool only, CA1-rflux, Empty and SX Ultra.

VII. Appendix: CO calibration curve

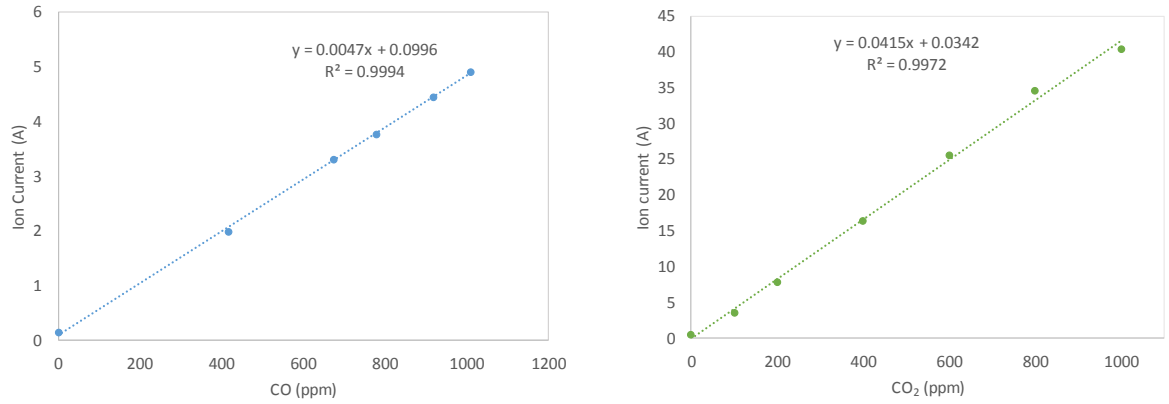

Figure 29. CO (left) and CO_2 (right) calibration curve used for the calculations of the CO concentrations measured during the TPD-MS.

VIII. Appendix: TPD profile of AC SX Ultra-ox. 12 % 0.5 h

In Figure 30 the TPD profiles of the different oxidized SX Ultra supports is show. It indicates that the SX Ultra oxidized with 12 % (v/v) HNO_3 for 0.5 h is in the same trend with the other oxidized carbons.

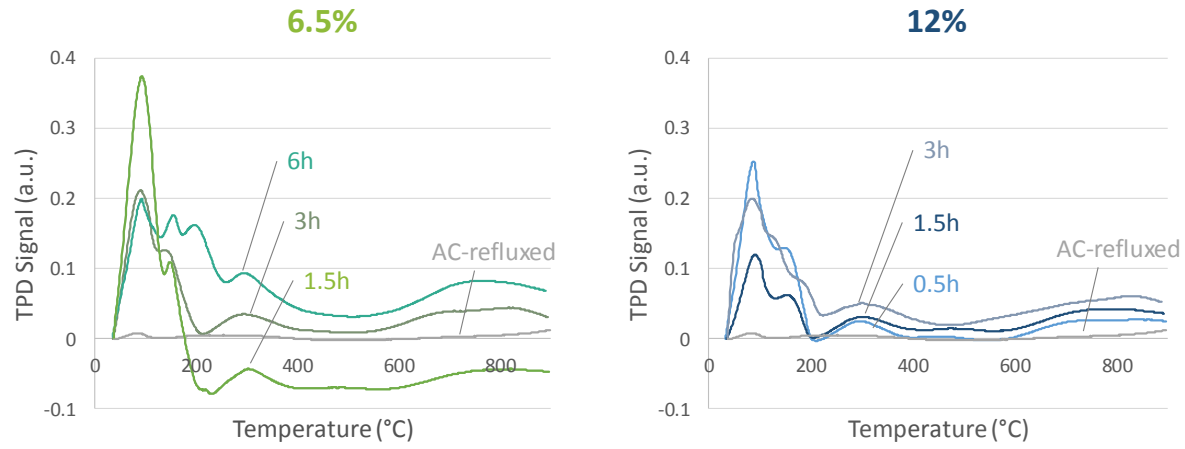

Figure 30. . TPD spectra of SX Ultra treated with 6.5% (green) and 12%(blue) at different treatment duration.

IX. Appendix: Glucose oxidation measured with Pt/AC-ox. 12 % 1.5 h

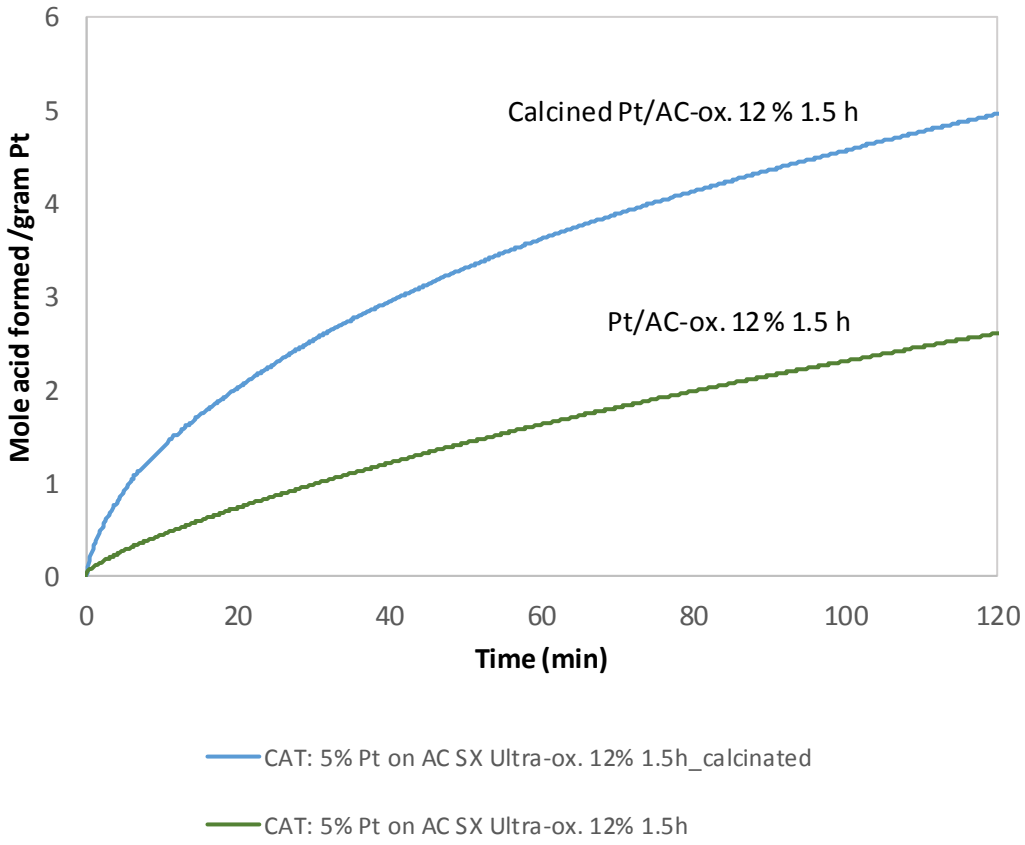

Figure 31. Glucose oxidation as measured by titration of formed acid. Catalyst used calcined and non-calcined Pt/AC catalyst supported on SX Ultra-ox. 12% 1.5 h. Reactions were performed at 50 °C, pH 9, 0.05 M substrate concentration, stirring speed of 2000 rpm and an oxygen flowrate of 300 mL/min.

X. Appendix: Precursor choice

Based on the hydrophilic or hydrophilic character of the support a desired precursor needs to be chosen. Support group with a high oxygen density were estimated to show a hydrophilic character, whereas the support without oxygen groups have less hydrophilic character. Therefore, support with a higher oxygen density were prepared with the $[Pt(NH_3)_4](NO_3)_2$. The catalyst derived from the H_2PtCl_6 precursor exhibits lower activity as can be seen in Figure 32 and was therefore not chosen.

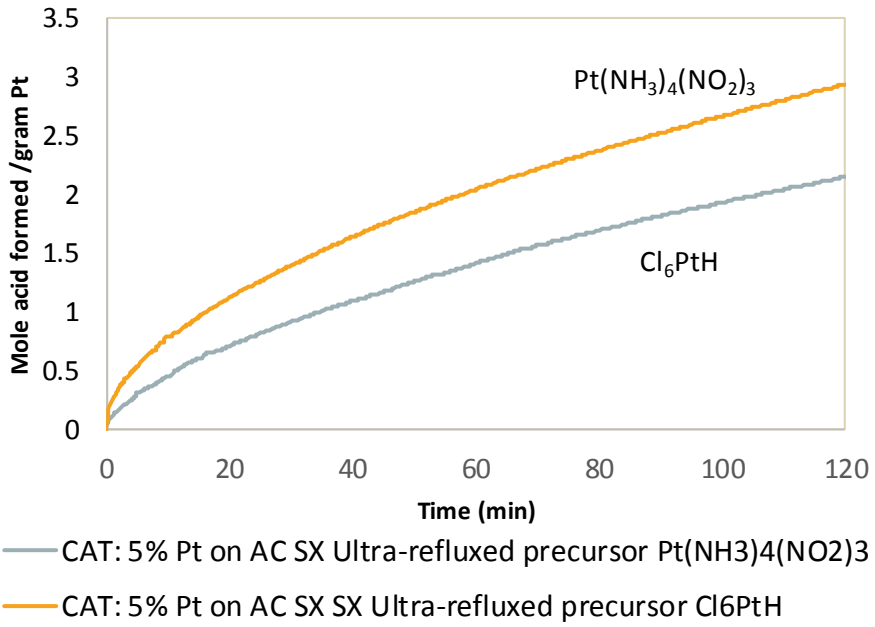

Figure 32. Glucose oxidation as measured by titration of formed acid. 5% Pt/AC catalyst supported on SX Ultra-reflux prepared with the precursor H2PtCl6 and $[Pt(NH_3)_4](NO_3)_2$ .Reactions were performed at 50 °C, pH 9, 0.05 M substrate concentration, stirring speed of 2000 rpm and an oxygen flowrate of 300 mL/min.

XI. Appendix: TEM images of the counted particles

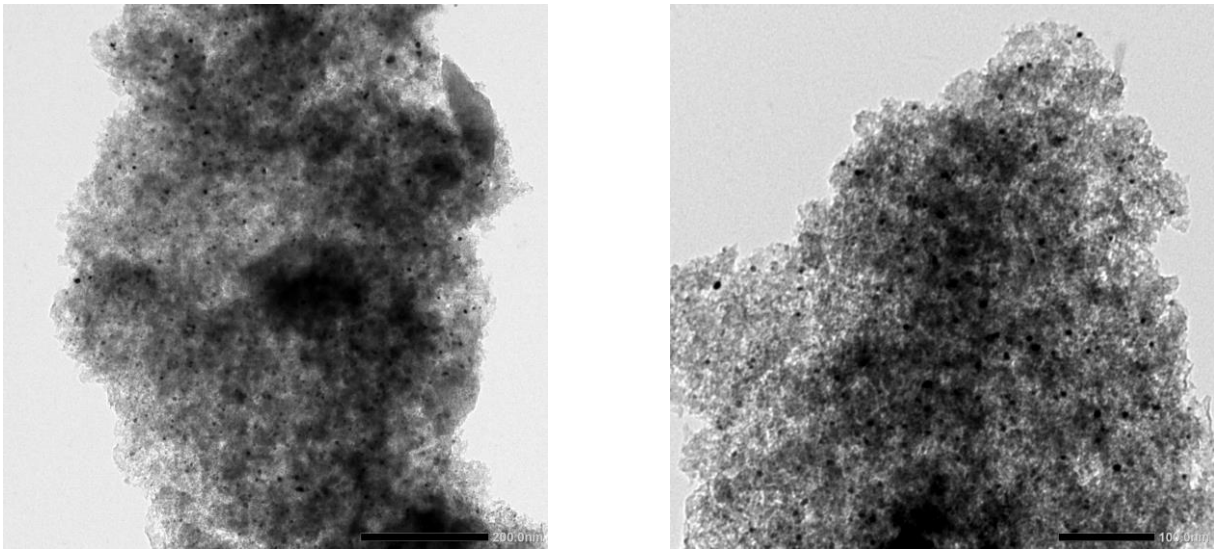

Figure 33. TEM images of the 5 wt.% Pt on AC SX Ultra-reflux.

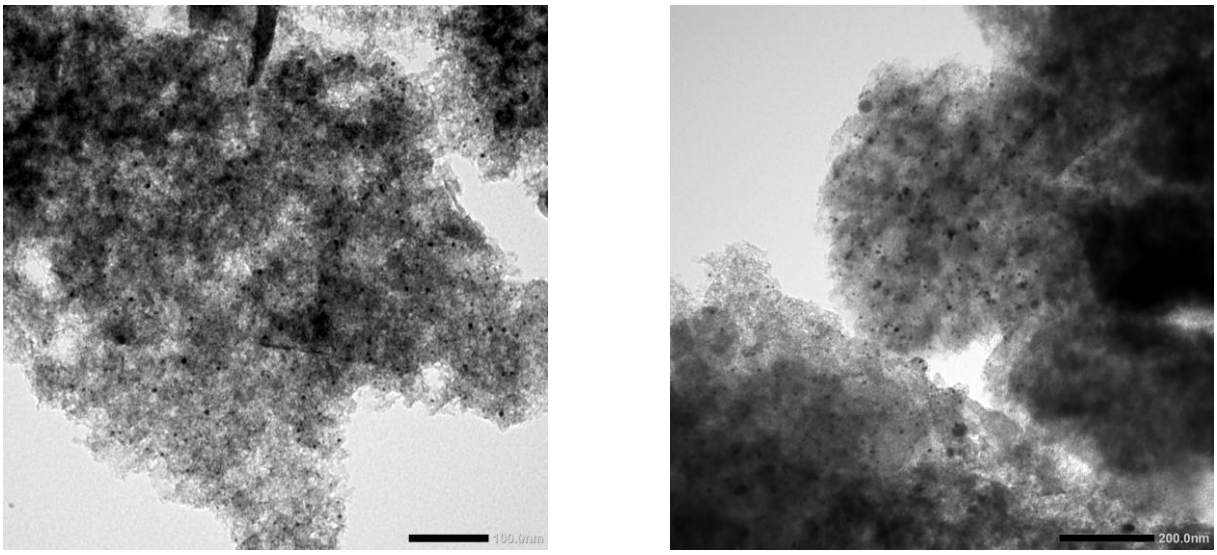

Figure 34. TEM images of the calcined 5 wt.% Pt on AC SX Ultra-reflux.

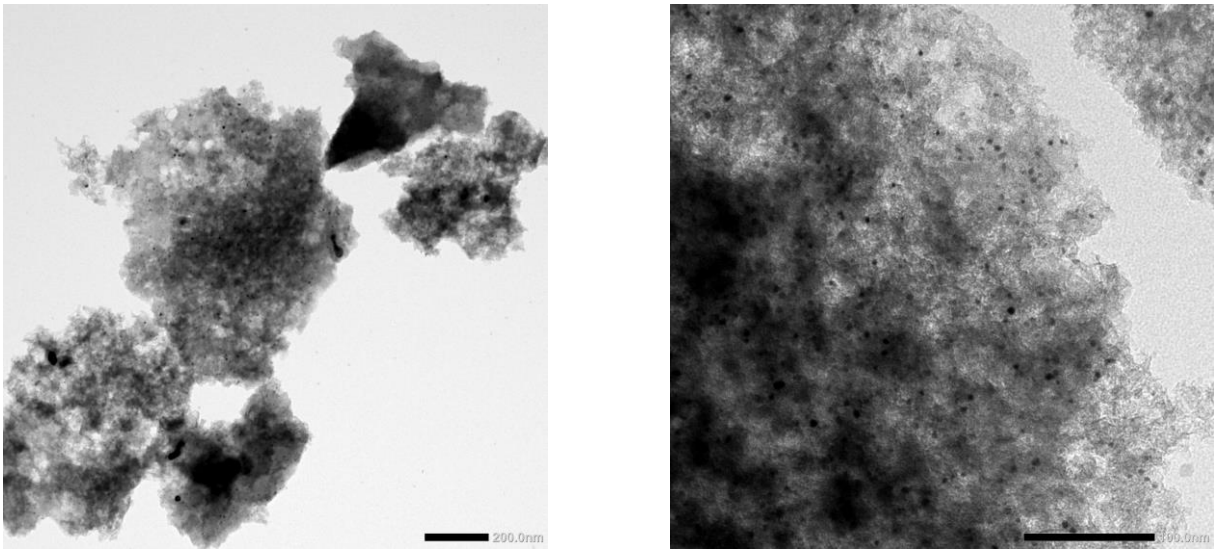

Figure 35. TEM images of the 5 wt.% Pt on AC SX Ultra oxidized with 6.5 (v/v)% HNO for 3 h.

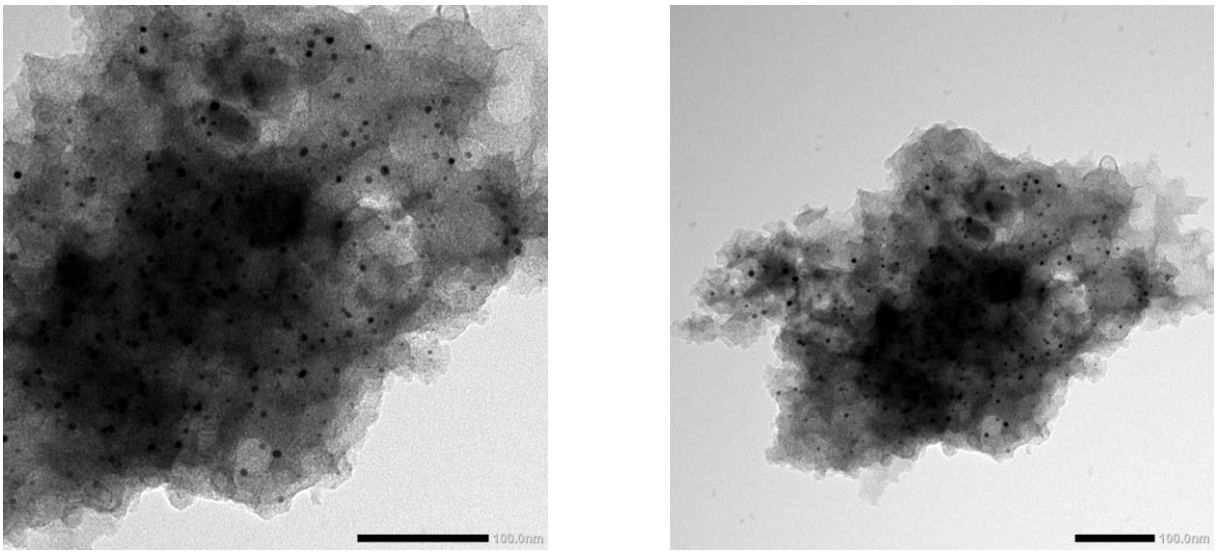

Figure 36. TEM images of the calcined 5 wt.% Pt on AC SX Ultra oxidized with 6.5 (v/v)% HNO for 3 h.

XII. Appendix: Pulse chemisorption data

Chemisorption data shown in Fig. was done with the reference sample (0.5% Pt on Al) – however, the chemisorption data does not result in the expected data of the reference.

Table 12. Pule Chemisorption data of the reference sample 0.5% Pt on Al. The CO chemisorption measurements were conducted at a reduction temperature at 350°C and 150°C. The CO chemisorption measurements were conducted in triplo at a reduction temperature of 150°C.

	CO		**H_2**		
	000-166_ Ref. 0.5% Pt on Al (CO-350C)	000-165_ Ref. 0.5% Pt on Al (CO150C)	000-169_ Ref. 0.5% Pt on Al (H2-150C) #1	000-170_ Ref. 0.5% Pt on Al (H2-150C) #2	000-171_ Ref. 0.5% Pt on Al (H2-150C) #3
Metal Dispersion:	54 %	70%	93%	89%	88%
Metallic Surface Area:	0.68 m^2/g sample	0.86 m^2/g sample	1.15 m^2/g sample	1.09 m^2/g sample	1.08 m^2/g sample
Metallic Surface Area:	136 m^2/g metal	172 m^2/g metal	231 m^2/g metal	219 m^2/g metal	216 m^2/g metal
Active Particle Diameter (hemisphere):	2.1 nm	1.6 nm	1.2 nm	1.3 nm	1.3 nm
Cubic Crystallite Size:	1.7 nm	1.4 nm	1.0 nm	1.1nm	1.1 nm

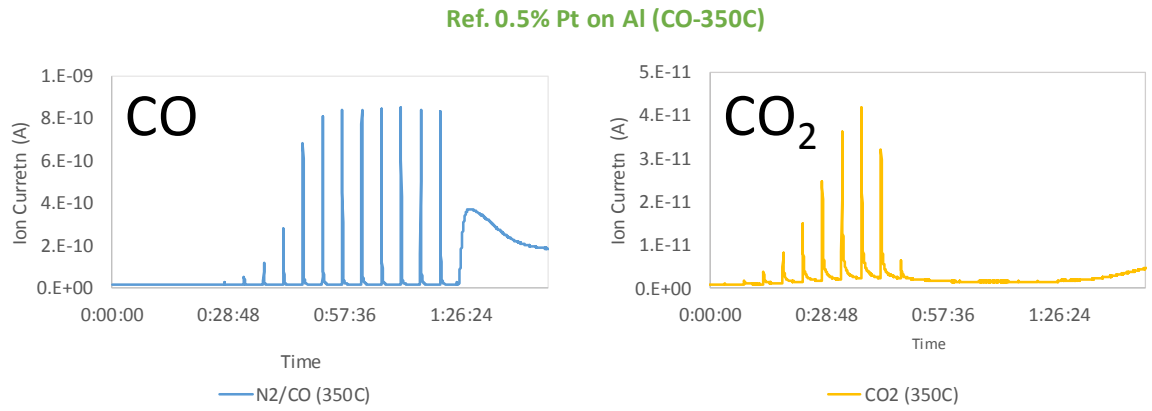

Figure 37. MS spectra of the CO Pulse Chemisorption measurements of 0.5% Pt on Al (reduction temperature 350°C). On the left the CO peaks and on the right the CO_2 peaks.

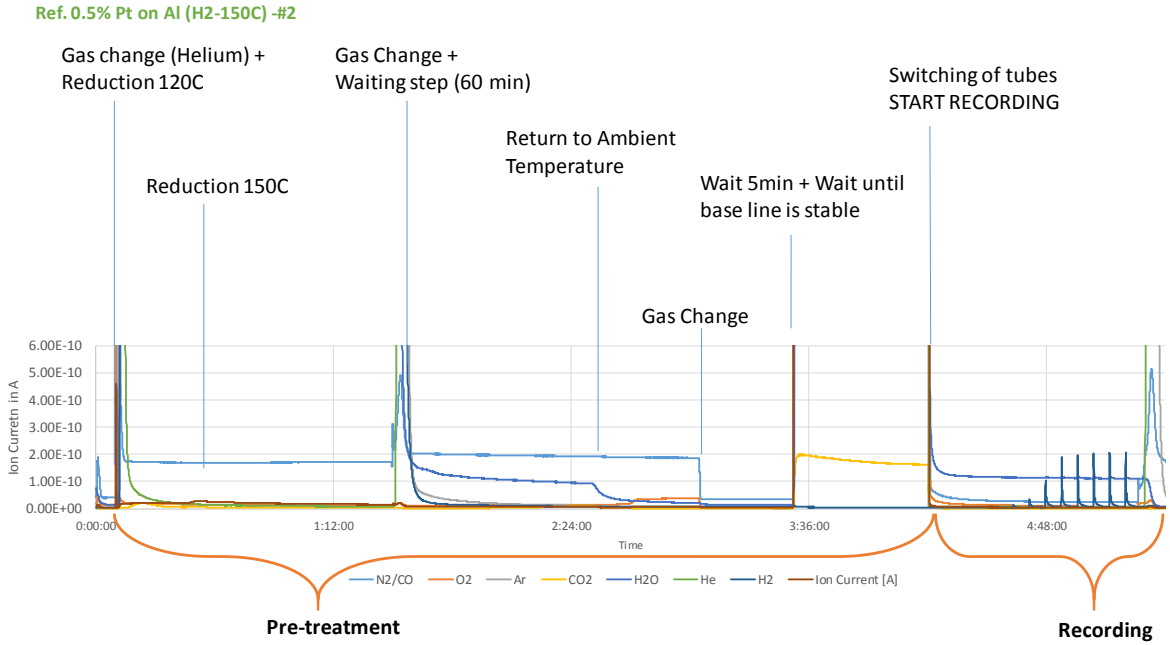

Figure 38. MS spectra of the H_2 Pulse Chemisorption measurements of 0.5% Pt on Al (reduction temperature 150°C). Explanation of each step during the pretreatment.

XIII. Appendix: Static chemisorption data

Table 13. Static Chemisorption data of the Pt particles of the 0.5 wt.% Pt on Al reference sample (reused and new) and the commercial catalyst with 5 wt.% Pt on AC.

	Reused Micromeritics Ref Mat 0.5% Pt on Alumina			**New Micromeritics Ref Mat 0.5%Pt on Alumina**	**Commercial catalyst 5 wt.% Pt on carbon**	
	#1	#2	#3			
Redcution Temperature	350	350	350	350	150	150
Crystallite Size (nm)	2.4	2.4	2.5	2.1	4.5	4.4
Metal Dispersion (%)	46.6	46.5	45.0	53.1	25.1	25.6
Quantity Adsorbed (µmol/g)	6.0	6.0	5.8	6.8	32.2	32.9

XIV. Appendix: HPLC chromatogram

The chromatogram shown in Figure 39 shows that the main peak results to Gluconic acid. Other possible produced acid acids, such as glucuronic acid cannot be detected from the chromatograms. As have been shown by my preassesor, the acids do not have the same retention time and are therefore not produced during the oxidation reaction.

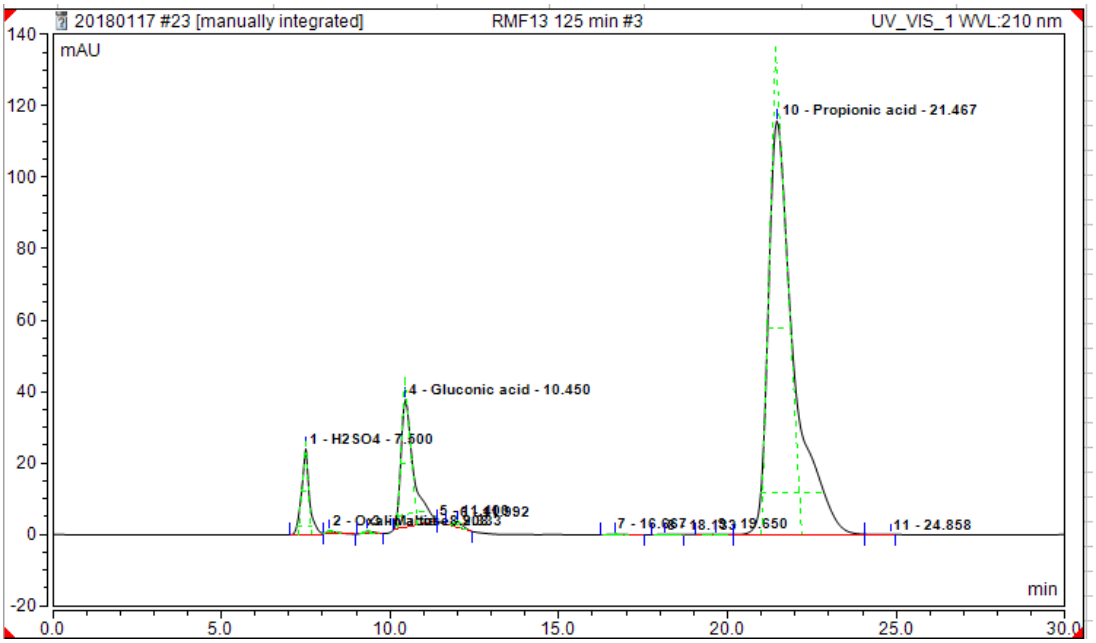

Figure 39. Represented HPCL Chromatogram of glucose oxidation catalyzed with 5 wt.% Pt/AC. It shows a clear gluconic acid peak at a retention time of 10-11 min.

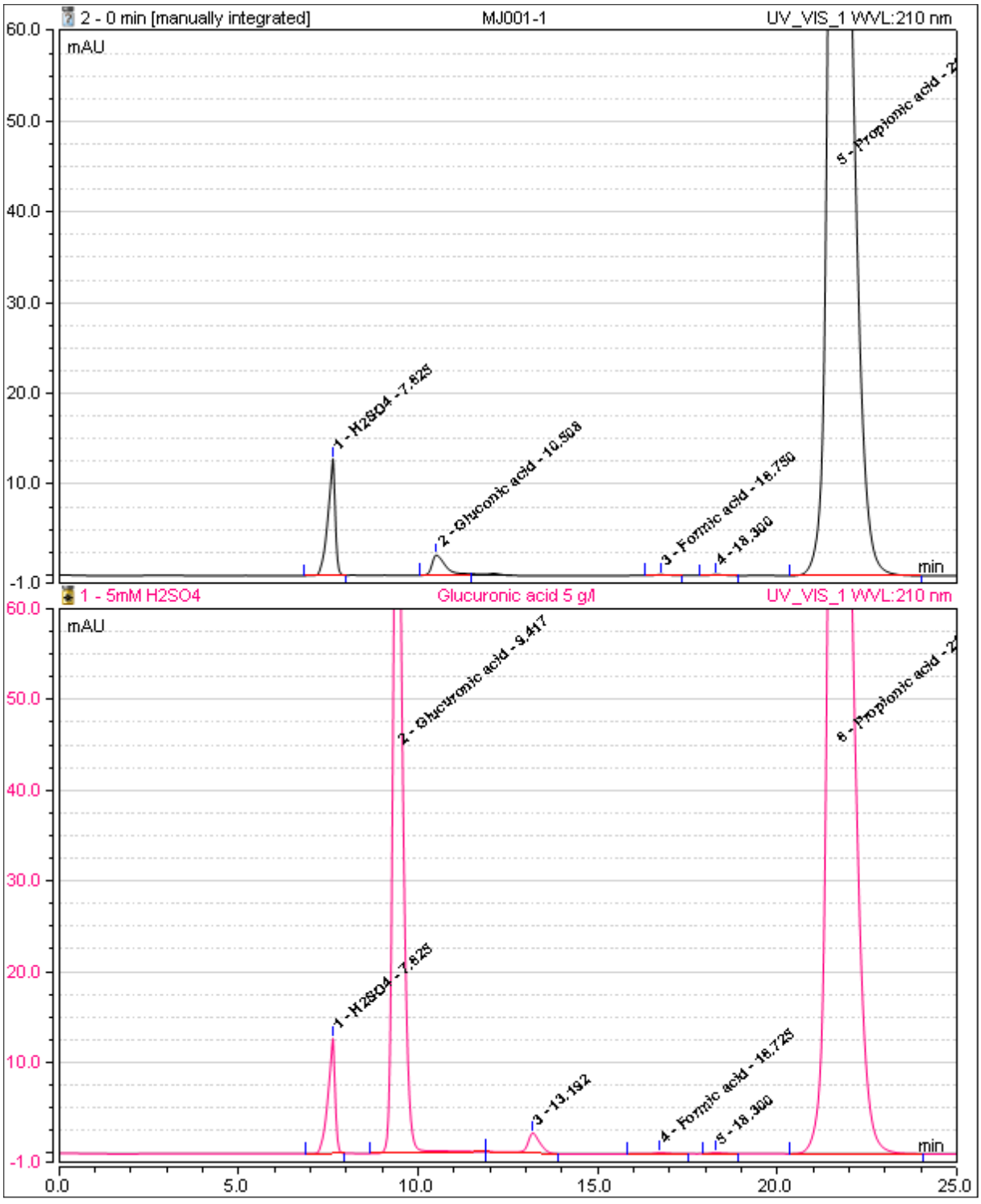

Figure 40. HPLC Chromatogram of gluconic acid (above) and glucuronic acid (down). The retention time of the gluconic acid was at 10-11 min and that of glucuronic acid at 9-10 min.